



Modelling the circulation on the continental shelf of the province Khanh Hoa in Vietnam

Knut Barthel^{a,*}, Rune Rosland^b, Ngoc Chien Thai^c

^a Geophysical Institute, University of Bergen, Allegaten 70, N-5007 Bergen, Norway

^b Department of Biology, University of Bergen, P.O. Box 7803, N-5020 Bergen, Norway

^c Research Institute of Aquaculture No. 3, 33 Dang Tat, Nha Trang, Vietnam

ARTICLE INFO

Article history:

Received 26 August 2008

Received in revised form 29 October 2008

Accepted 11 November 2008

Available online 30 November 2008

Keywords:

Ocean circulation

Flushing time

Wind-driven currents

Continental shelves

Time-dependent forcing

Vietnam

12–13°N, 109°E

ABSTRACT

A model simulation of the circulation on the continental shelf of the Khanh Hoa province in central Vietnam during the year 2004 is presented. The model, a three-dimensional baroclinic z -coordinate model (the Hamburg Shelf Ocean Model), is implemented with a horizontal resolution of about 1 km. It is initialised with temperature and salinity fields taken from the Levitus data, and by the two main tidal constituents. The model is forced by daily fields of wind stress, air temperature, wind speed, and cloudiness taken from NCEP, and by monthly mean river runoff values. At the open boundary sea surface displacements are prescribed by the tidal variation and by the steric height determined from the density anomalies determined from climatological values of temperature and salinity.

The modelled circulation reflects the monsoonal forcing fields, and reveals downwelling during winter and upwelling during summer. The modelled hydrography is compared with measured profiles, and some biases are found. The flushing times of three bays along the Khanh Hoa coast are calculated. The relative influence of river runoff, tides, and weather on the flushing times is discussed.

© 2008 Elsevier B.V. All rights reserved.

1. Introduction

The width of the continental shelf varies a lot along the coast of Vietnam. The shelf of the Khanh Hoa province, located between 12°N and 13°N, is narrow, and depth increases steeply to several thousands meters (Fig. 1).

The coast of Khanh Hoa (Fig. 2) includes some large shallow bays that are utilised for pond based aquaculture and sea based cage farming. Van Phong Bay in the northern part has a mean depth of about 15 m and covers about 510 km². Many small rivers flow into this bay, but no large ones. In the northern central part is the Nha Phu Bay, which is less than 10 m deep and covers 104 km². At the end of the bay a main river system (Dinh, Tan Thuy, Da Han) discharges about 30 m³/s in the wet season (Table 1). Nha Trang Bay in the

central part has about the same size as Nha Phu Bay, but it is deeper and more exposed to the open sea. Cai River flows into this bay and discharges about 460 m³/s (Table 1) in the wet season. Cam Ranh Bay, which is located about 40 km south of Nha Trang city, is semi-enclosed and has a mean depth of 10 m and covers 119 km².

The area has a monsoon weather regime; the wet season lasts from July to December with an average rainfall about 1300 mm/yr. The dry season lasts from January to May. The monsoon regime has a strong impact on the ocean circulation along the coast of Vietnam, which changes from a southwest flow during winter to a northeast flow during summer (Wyrтки, 1961), (Shaw and Chao, 1994). Coastal upwelling occurs during summer. The tropical climate and the upwelling make the conditions favourable to aquaculture and fishing (An and Thu, 2007).

The Vietnamese coast is characterised by extensive fisheries and aquaculture production (An and Thu, 2007). Aquaculture is an increasingly important export industry in Vietnam and the government runs an active policy to stimulate growth and

* Corresponding author. Tel.: +47 55582887; fax: +47 55589883.
E-mail addresses: knut.barthel@gf.uib.no (K. Barthel),
rune.rosland@bio.uib.no (R. Rosland), thaichienfish@yahoo.com (N.C. Thai).

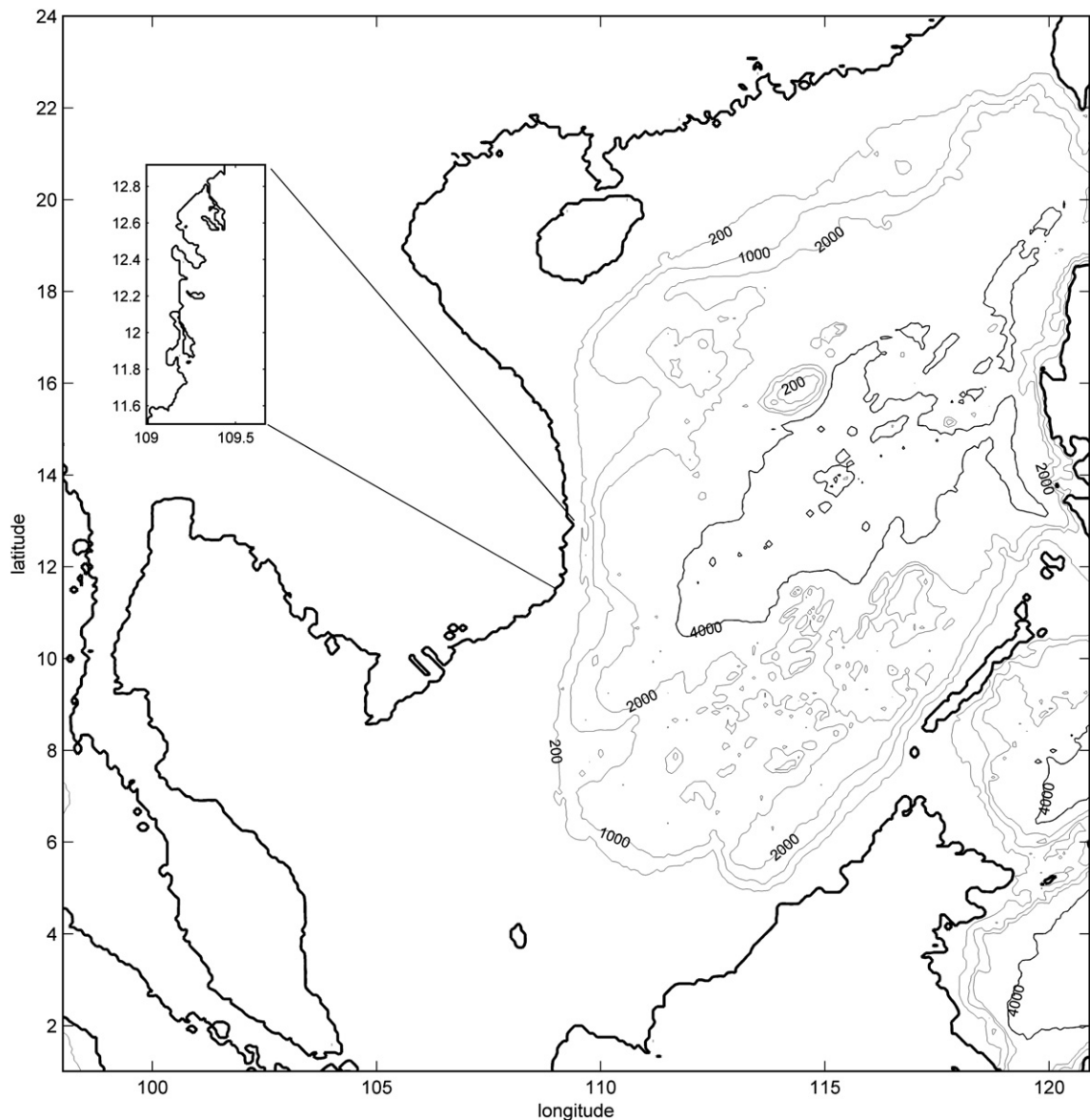


Fig. 1. Bathymetry of South China Sea in meters (derived from the ETOPO5 database, (Hirtzler, 1985)). The model region is indicated by the inserted map.

expansion of the aquaculture industry. This implies a shift from extensive to intensive farming systems and extended use of available water bodies. Intensive farming usually implies more discharges of inorganic nutrients and organic material to the surrounding water bodies. Combined with an expansion of production areas this may cause a significant increase in the discharges to the coastal marine system. Development of pond based aquaculture has caused destruction of mangrove forests and other wetland systems with important filtering capacity for water running into the marine system. Today, some of the regions that are densely populated with shrimp farms experience problems with organic loads and bad water quality (An and Thu, 2007). Apart from the negative effect on local flora and fauna, bad

water quality may also hit back on the aquaculture systems in terms of increased mortality, reduced production and quality of the products. Considering today's problems and awareness of the future development of aquaculture in Vietnam it is important to increase knowledge about the state of the bays and their carrying capacities, which are measured by the flushing time.

This paper presents the application of a three-dimensional shelf-ocean model on the coast of the Khanh Hoa province. We focus on the circulation in the bays, and how it responds to varying wind forcing. The research objectives are to quantify water exchange and to identify important driving forces on the system. The modelled hydrography, current, and vertical mixing fields will be used to force a primary production model

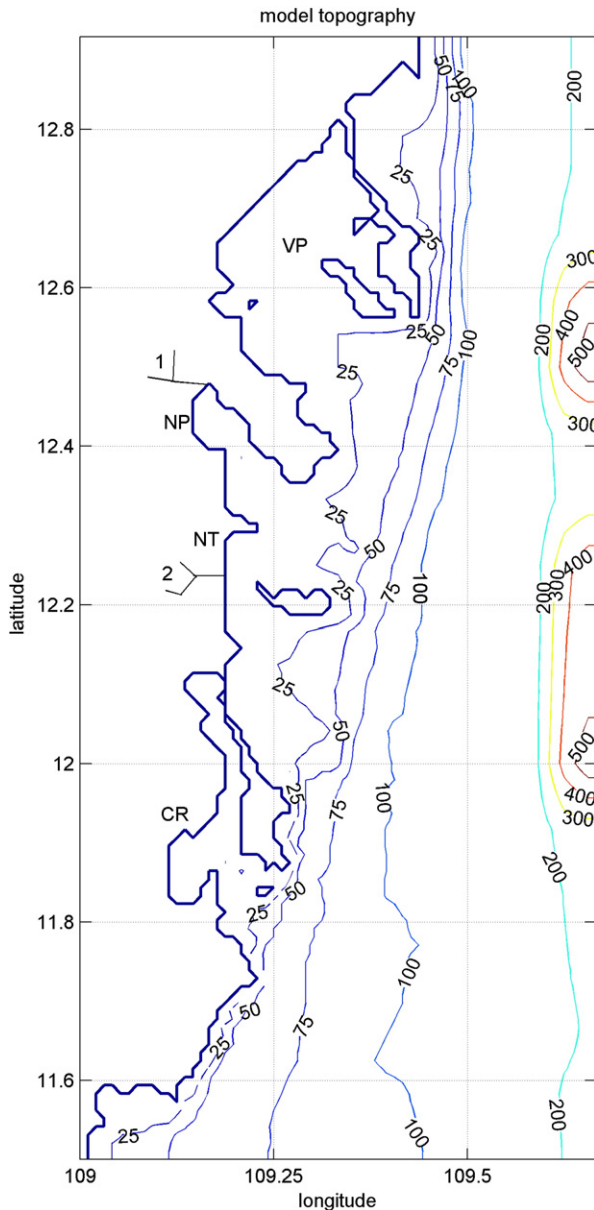


Fig. 2. Bathymetry of the coast of Khanh Hoa province, in meters (derived from Vietnamese sea charts and ETOPO5). VP=Van Phong Bay, NP=Nha Phu Bay, NT=Nha Trang Bay, CR=Cam Ranh Bay, 1=Dinh, Tan Thuy, and Nga Hau rivers, 2=Cai river.

which is presented in another paper (Thai et al., submitted for publication). We will discuss physical processes with relevance for aquaculture production and development, and present validation measures relating model performance to field observations from the area.

2. Methods

The model applied here is the Hamburg shelf-ocean model (HAMSOM), which was developed by Backhaus at the

University of Hamburg. This model has been applied in several continental shelf studies around the world, and also for the South China Sea (Pohlmann, 1987). Results of the applications can be found in papers like (Schrum, 1997), (Hainbucher et al., 2004), and (Barthel et al., 2004).

The implicit treatment of the external gravity waves in this model allows for a longer time step (Backhaus, 1983). Hence, instead of a time step of 10 s, as would be necessary for numerical stability with a pure explicit treatment, we can use a time step of 150 s. The numerical scheme used for the time integration of the hydrodynamic equations is described in (Backhaus, 1985).

The model is a z-level model, and in this study we apply a configuration of 12 layers with lower boundaries at 2, 5, 10, 20, 30, 50, 80, 120, 200, 300, 450, and 615 m. Horizontally the model region (109°E to 109°40'E, 11°30'N to 12°55'N) is divided into cells of 37.5'' both in latitudinal and longitudinal direction, giving a grid distance of a little more than 1 km. The Arakawa C-grid is used.

Forced by winds, tides and air–sea heat fluxes the model was run for the year 2004. Daily NCEP reanalysis data (Kalnay et al., 1996) with 1.9° resolution were interpolated to the model grid. The time series of wind stress at the NCEP point 110.6°E, 12.4°N is shown in Fig. 3. The time series reflect the general picture of the monsoon wind system in the South China Sea, with a strong north-easterly wind in the winter season and a weaker south-westerly wind during summer, as described in Liu et al. (2001).

A 1 year spin-up run from climatological values of temperature and salinity (Conkright, et al., 2002), (Levitus, 1982) was done before the simulation. Along the open boundaries temperature and salinity were prescribed by seasonal climatological values, and phase and amplitude of the main tidal constituents (K1 and M2) were prescribed by use of tidal maps and a report by Bui and Tran (2005). From these data the sea surface displacement along the open boundaries was determined. The steric height was determined from the salinity and temperature through the nonlinear density formulation of Fofonoff and Millard, (1983). Model work similar to this has been done in the Bohai Sea (Hainbucher et al., 2004), where HAMSOM was implemented in the same way as in this study regarding open boundary conditions. The Neumann condition with zero gradient normal to the open boundary is standard for this model, but led to a drift away from climatological values of temperature and salinity here. Therefore a Dirichlet condition with open boundary values fixed to a seasonal climatology was applied.

Two river discharges are taken into account, one at Nha Phu Bay (Dinh River) and one at Nha Trang (Cai River), see Fig. 2. The discharges vary with the season according to the monsoonal shift and the values used (Bui Hong Long, personal communication) are given in Table 1. They represent climatological values.

Table 1
River discharges in m³/s used in the simulation (Bui, personal communication).

	Jan	Feb	Mar	Apr	May	Jun	Jul	Aug	Sep	Oct	Nov	Dec
Dinh	15	15	15	14	16	20	21	29	30	30	30	23
Cai	230	230	230	207	239	299	327	437	460	460	460	345

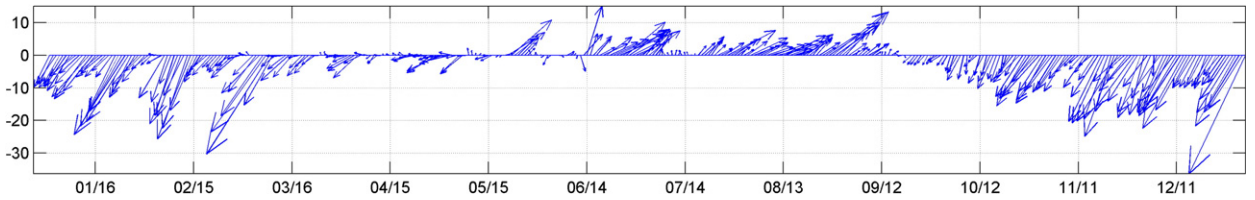


Fig. 3. Time series of NCEP wind stress at 110.6°E, 12.4°N, year 2004. Arrow direction represents the wind direction (an arrow straight downwards is a North wind) and arrow length represents the wind stress magnitude (cPa).

The model computes sea surface displacement, transports, 3D velocities, temperature, salinity, and sea surface radiation. Also, the vertical eddy viscosity coefficient is computed, based

on a method by (Kochergin, 1987) and later modified by (Pohlmann, 1996). The vertical eddy viscosity coefficients depend on stratification and vertical shear of the current, and

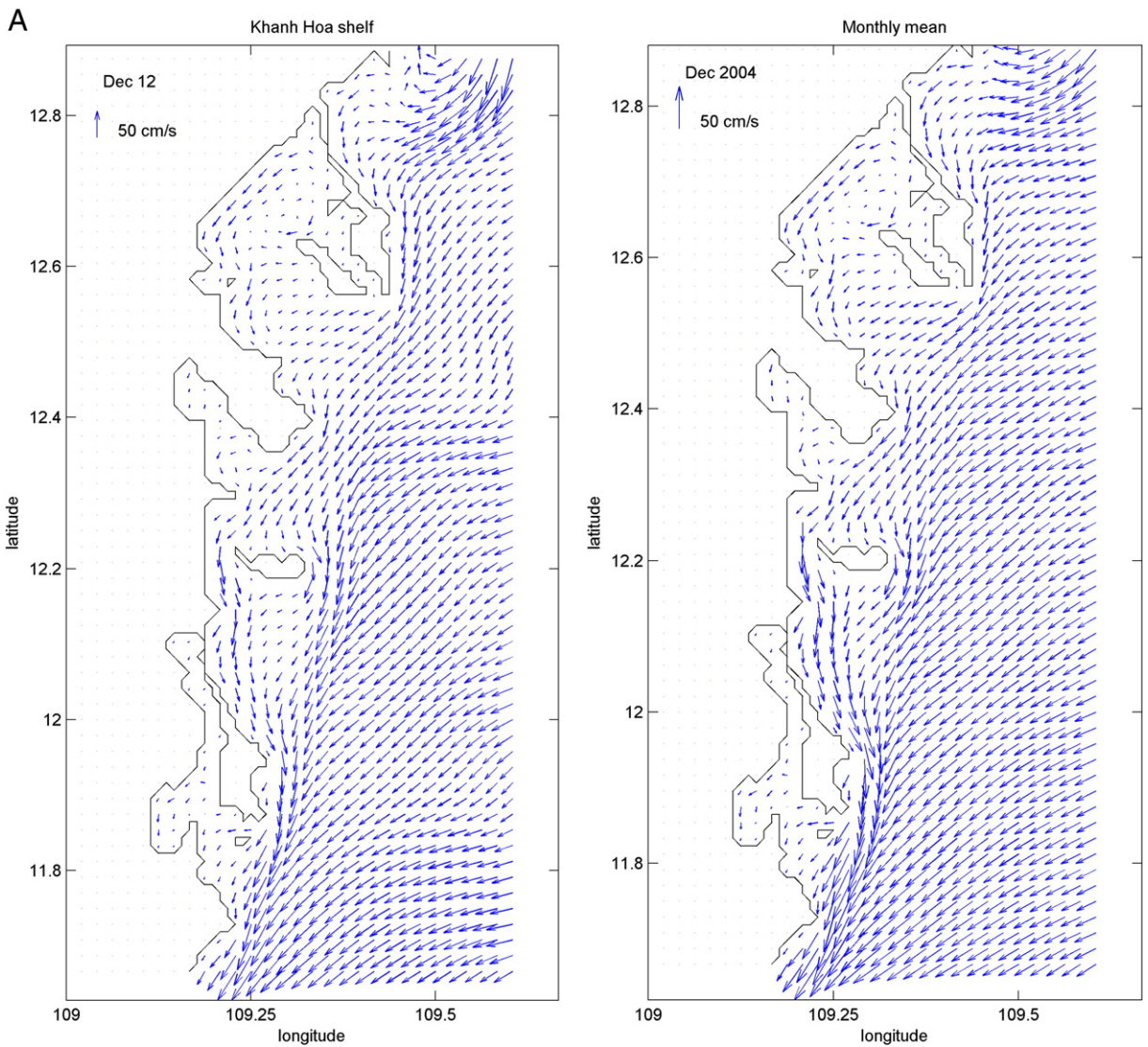


Fig. 4. A. Daily mean surface current (cm/s) of 12 December 2004 (left panel). Monthly mean surface current of December 2004 (right panel). B. Daily mean surface current (cm/s) of 12 December 2004 in Nha Trang Bay (left panel) and Van Phong Bay (right panel). C. Daily mean surface current (cm/s) of 12 December 2004 in Nha Phu Bay (left panel) and Cam Ranh Bay (right panel). (The currents outside Cam Ranh Bay, which are much stronger, have been set to zero to get a view of the field inside the bay.). D. Vertical mean current of 12 December 2004 (left panel). Monthly mean of the vertical mean current of December 2004 (right panel). E. Vertical mean current of 12 December 2004 in Nha Trang Bay (left panel) and Van Phong Bay (right panel). F. Vertical mean current of 12 December 2004 in Nha Phu Bay (left panel) and Cam Ranh Bay (right panel). (The currents outside Cam Ranh Bay, which are much stronger, have been set to zero to get a view of the field inside the bay.)

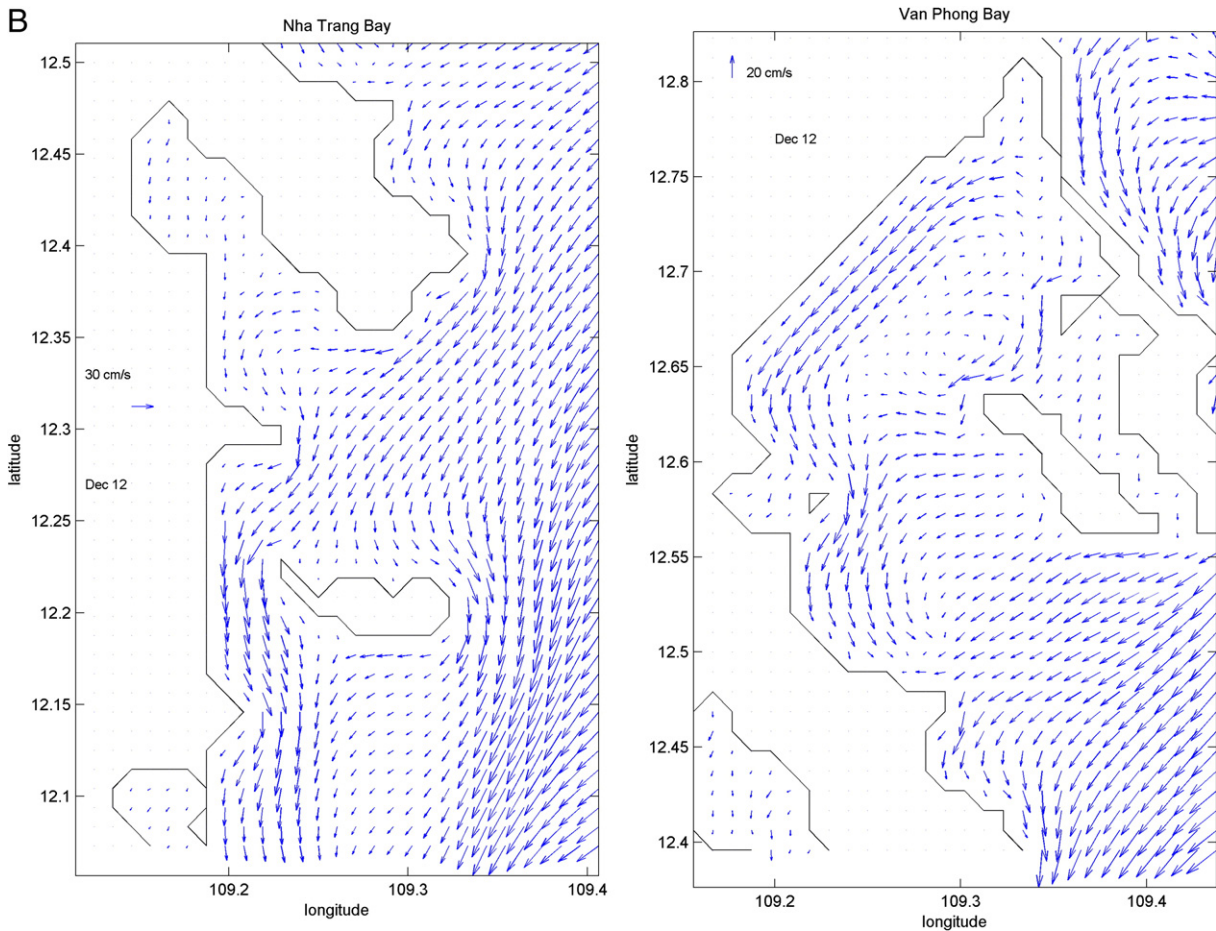


Fig. 4 (continued).

the method is related to the level-2-model of (Mellor and Yamada, 1974).

3. Results

The left panel of Fig. 4A shows the modelled daily mean surface current field for 12 December 2004, and the right panel shows the mean surface current field for the same month.

The circulation of 12 December is representative for this winter month. The flow is southwards along the coast with a substantial onshore component. The typical current value is about 1 knot. Outside the shallow bays there is a strong confluence region which is setting up a strong southward current. Signs of coastal downwelling are seen in the vertical temperature distribution for a section running eastwards from the tip of the Cam Ranh peninsula (Fig. 5). The figure shows warmer water that is brought downwards near the shore. The 22 °C isotherm has the largest slope. Fig. 4B and C display the surface currents for the same day in the bays of Nha Trang and Van Phong (4b), and Nha Phu and Cam Ranh (4c). The near shore flow is rather strong with a southward component. Several eddies are seen in Van Phong bay, and the island Hon Tre outside Nha Trang creates a wake in the

southward flow. The water from Cai River is deflected southwards and keeps close to the shore. Both in Nha Phu bay and in Cam Ranh bay the surface circulation is steered by the prevailing north-easterly wind. The vertical mean current fields for the same day and month are shown in Fig. 4D. There is a strong southward jet outside the bays. Eddies in the bays are displayed more clearly by the vertical mean circulation fields (Fig. 4E–F).

The surface current during the summer season, here represented by the daily mean of 5 September 2004 and the mean for the same month, is completely different, (Fig. 6A), with a northward flow along the coast, and a mainly off-shore component. The shelf current meanders strongly, and there is a weaker counter-current inside of it, that takes the water from Nha Trang bay into a southward loop before it merges with the shelf current and flows northward. The speeds are somewhat stronger than during winter. This circulation is connected with coastal upwelling, displayed by the vertical temperature distribution seen in Fig. 7. Cooler water beneath the surface layer is brought upwards near the shore. Fig. 6B and C display the surface currents for the same day in the bays of Nha Trang and Van Phong (6B), and Nha Phu and Cam Ranh (6C). In Nha Trang Bay (Fig. 6B, left panel) the flow is directed off shore, and we see a strong divergence

C

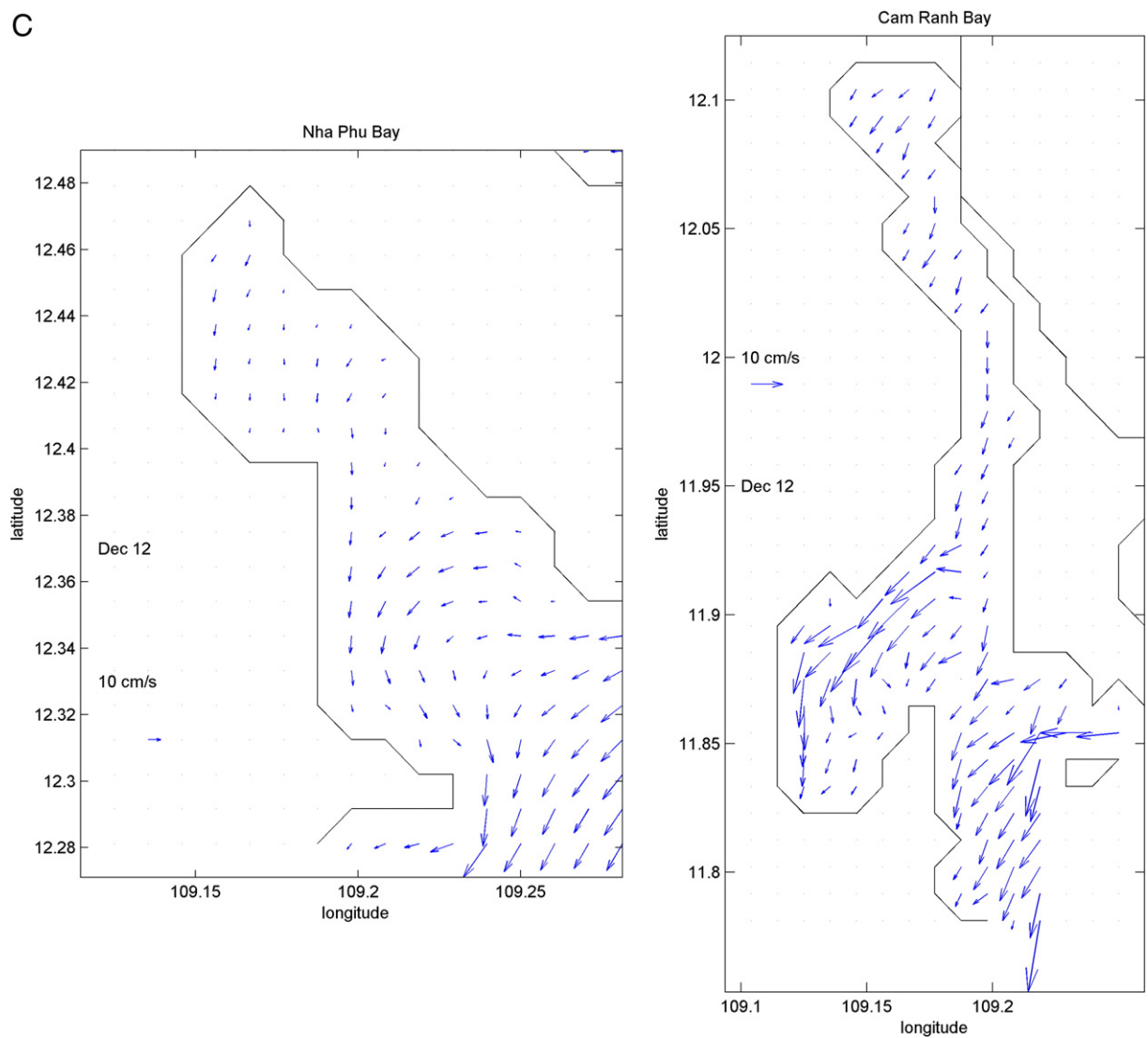


Fig. 4 (continued).

at the mouth of Cai River (12.25°N). In Van Phong Bay the circulation on 5 September 2004 (Fig. 6B, right panel) is opposite to what it is on 12 December (Fig. 4B, right panel). In Nha Phu Bay the surface circulation is directed outwards (Fig. 6C, left panel), but it follows the eastern shore during September, and the western shore during December (compare with Fig. 4C, left panel). Also in Cam Ranh Bay the circulation is opposite on 5 September to what it is on 12 December (compare right panels of Figs. 6C and 4C). The vertical mean circulation for the same day and month looks quite similar to the surface circulation; compare Fig. 6D and A. But the vertical mean circulations in the bays differ a lot from the surface circulation; compare Fig. 6E–F and B–C. Although winds are stronger during December than during September, the current speeds are stronger during September, because the steric height slope is stronger; compare Figs. 6D and 4D.

Fig. 8A shows vertical profiles of observed and modelled temperature at the mouth of Cam Ranh Bay ($109^{\circ}12'04''\text{E}$, $11^{\circ}52'26''\text{N}$, see inserted map for site location). The mean values are displayed together with standard deviations which are based on 21 profiles taken at 4 h intervals during the period 9 to 12 March 2004. The observed and modelled salinity profiles from the same location and period are displayed in Fig. 8B.

The observed temperatures lie between 24 and 25.5°C , while the modelled ones are 1 to 1.5°C higher. The modelled salinities are 0.2 to 0.3 too low, when compared to the observations. The diurnal variation reflected by the standard deviations is similar for the observed and modelled temperature. The observed surface temperature varies about 1°C , while the modelled temperature shows less variation. In the deeper layers from 10 m and downwards the observed and modelled temperatures vary by the same amount. Modelled

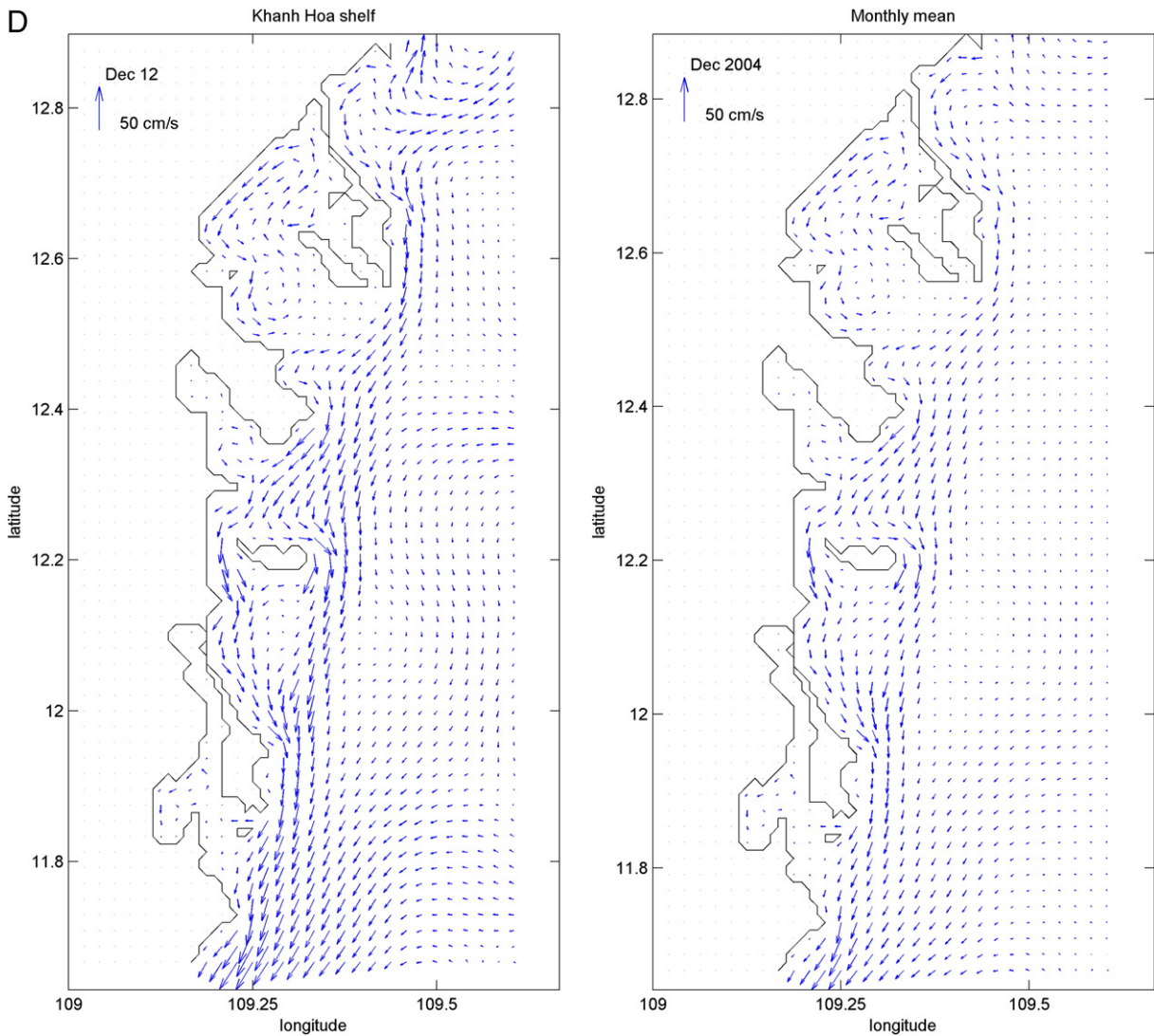


Fig. 4 (continued).

salinity varies by 0.1 at all depths down to 20 m, while observed salinity varies by 0.1 at the surface and 0.05 at the bottom.

To compare modelled and observed stratification, time series of temperature and salinity differences between 3.5 m and 7.5 m depth at the same place are displayed in Fig. 9. The modelled data, which represent the period from 1 to 13 March 2004, show a period of 120 h of low stratification just before and during the period when the observations were made. The agreement between observations and model results are quite good with respect to the onset and magnitude of the stratification. The period of low stratification coincides with a 5 day gale event (see Fig. 3, between 02/15 and 03/16) which gives a well mixed upper ocean due to mechanical stirring.

Fig. 10A shows vertical profiles of observed and modelled temperature at the mouth of Van Phong Bay (109°22′29″E,

12°32′08″N, see inserted map for site location). The mean values are displayed together with standard deviations which are based on 7 profiles taken at 4 h intervals during the period 2 to 3 March 2004. The observed and modelled salinity profiles from the same location and period are displayed in Fig. 10B.

The observed mean temperature is 25.4 °C in the upper 5 m, and varies by almost 0.5 °C. The modelled mean temperature is 2° higher in this upper layer, and varies also by about a half degree. From 5 to 12 m depth the observed temperature drops below 23 °C and remains relatively constant down to the bottom, while the modelled temperatures drop gradually down to 25.4 °C at the bottom.

The observed salinity profile (left panel of Fig. 10B) has a stratification resembling that of the observed temperature. The values are constant in the upper 5 m, then the salinity increases relatively quickly the next 9 m, and thereafter more

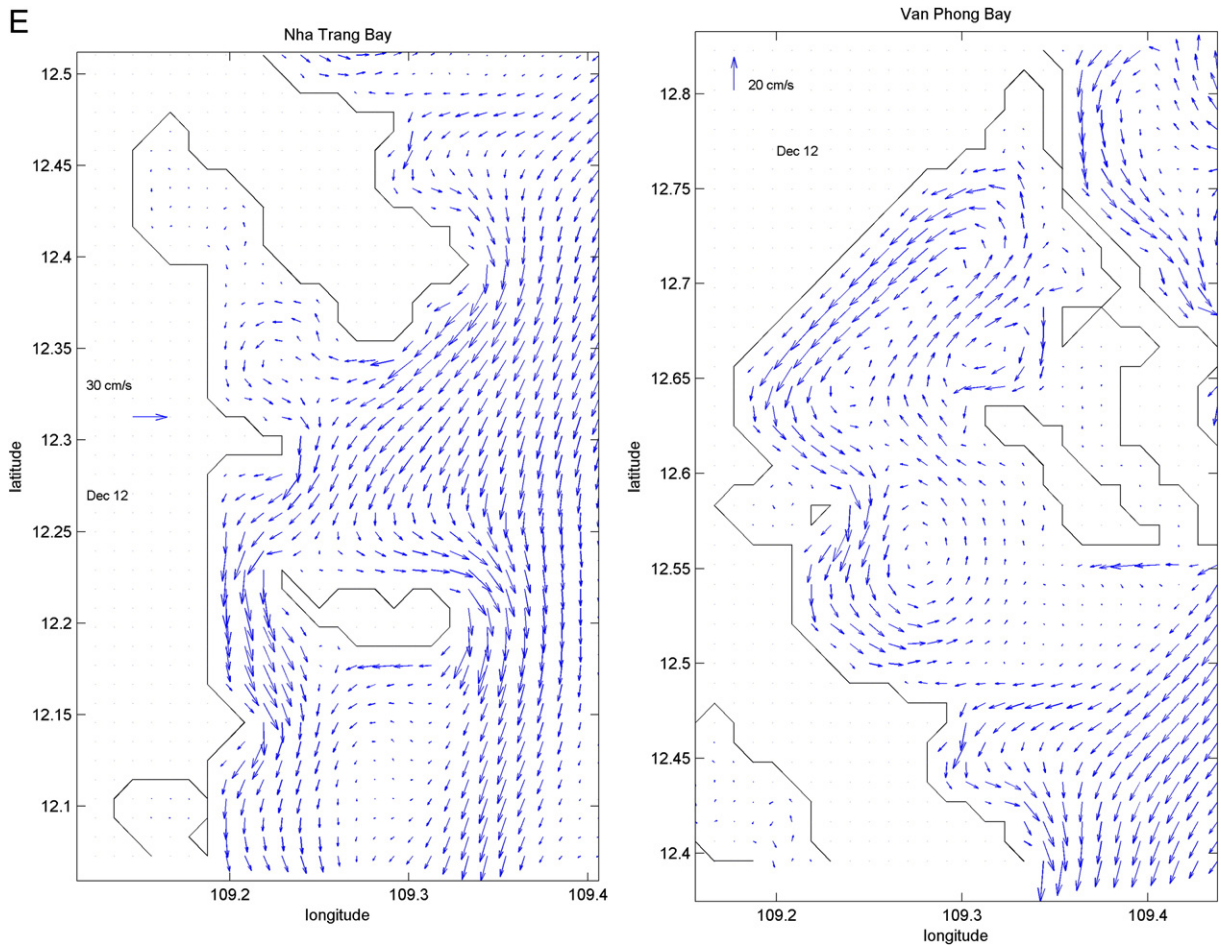


Fig. 4 (continued).

slowly down to the bottom. The standard deviation is large (about 0.1) at 6 m and 12 m, and smaller (about 0.03) elsewhere. The modelled salinity is quite constant with depth (right panel of Fig. 10B). The model sea is too salty at the surface, and too fresh at the bottom at this site. The diurnal variation is almost zero.

The calculations of the flushing times of Van Phong Bay, Nha Phu Bay and Cam Ranh Bay are based on the tidally resolved transport, which means that the flow across the open bay boundary is calculated at each time step. This estimate of the flushing time is a theoretical lower value, because it assumes that the in-flowing water becomes fully mixed before it leaves the bay.

The open boundaries of the bays applied for these calculations are shown in Fig. 11. The water volumes inside these boundaries are 1.838, 0.541, and 1.719 km³ for Van Phong Bay, Nha Phu Bay and Cam Ranh Bay, respectively. If Q is the in-flowing transport, the flushing time, T , is calculated by $T = V/Q$, where V is the water volume.

The average flushing time for Van Phong Bay's inner part as defined by boundary No.1 in Fig. 11, is 9 days. The upper panel of Fig. 12 displays a clear seasonal variation, with short

flushing times of 7–8 days in January, February, November, and December, and longer times of about 11 days during April to September. The variance is large in winter and small in summer.

The average flushing time for Nha Phu Bay as defined by boundary No.2 in Fig. 11, is 4.5 days, see mid panel of Fig. 12. Here the shorter flushing times of 3.3 days are found during August, while the longer times of 5.0–5.5 days are found in the winter months with a peak in the driest month April.

The average flushing time for Cam Ranh Bay as defined by boundary No.3 in Fig. 11, is 6 days, see lower panel of Fig. 12. Here the shorter flushing times are during the dry season, and the strongest variation of the flushing times is during April to July.

The mixing conditions can be examined by studying the results for the vertical eddy viscosity. Time series of the modelled values at 3.5 m for the four locations given in Fig. 11 are displayed in Fig. 13. At the mouth of Van Phong Bay (upper panel, same as the observation site displayed in Fig. 10) there is a strong seasonality with little mixing from mid April to the end of September, and periods of strong mixing reaching values of 0.036 m²/s during the winter months. At the Nha Phu Bay site (second panel from top) the

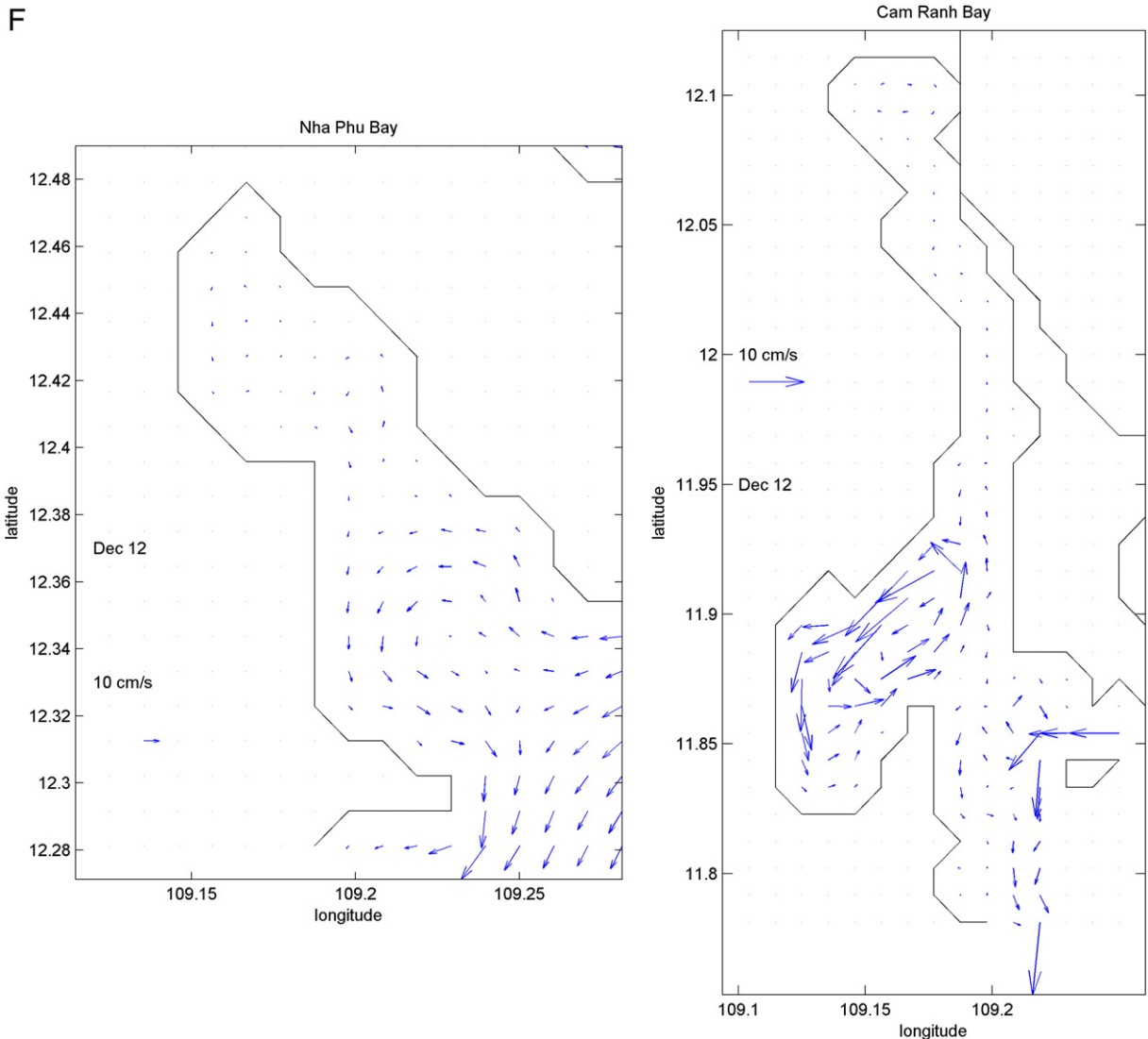


Fig. 4 (continued).

mixing conditions do not show any seasonality, and stay quite low at a value around $0.002 \text{ m}^2/\text{s}$. At the site in Cam Ranh Bay (third panel from top, same as the observation site displayed in Fig. 8) there is rather strong mixing the whole year, but with a quiet period from May to August. The average value $0.006 \text{ m}^2/\text{s}$ is the same as at the site in Van Phong Bay. The maximum value is $0.022 \text{ m}^2/\text{s}$. The fourth site which is south of the island Hon Tre in Nha Trang Bay (lower panel), has mixing values above $0.01 \text{ m}^2/\text{s}$ during the winter months, and during the rest of the year the values are only around $0.002 \text{ m}^2/\text{s}$.

The spatial distributions of the mixing conditions for the summer season and for the winter season are given in Fig. 14, left and right panel, respectively. The monthly mean values for September reveal some local maxima in the inner Van Phong Bay reaching above $0.004 \text{ m}^2/\text{s}$. Also in Cam Ranh Bay and at the mouth of Nha Phu Bay there are local maxima. The

winter season circulation gives strong currents and strong mixing conditions outside the bays, so that eddy coefficients are reaching monthly mean values of nearly $0.04 \text{ m}^2/\text{s}$. In the bays the overall values are increased by about a factor two compared to the summer season values.

4. Discussion

The modelled hydrography at the mouth of Van Phong Bay seems to be too homogeneous with respect to observations, which show a strong stratification with temperatures ranging from $25.5 \text{ }^\circ\text{C}$ at 5 m to $23 \text{ }^\circ\text{C}$ at 10 m. The climatological values used for the open boundaries have a much deeper thermocline, so that the temperature does not become less than $23 \text{ }^\circ\text{C}$ until below 80 m.

At the mouth of Cam Ranh Bay, the observations show less stratification, and there the modelled values match better to

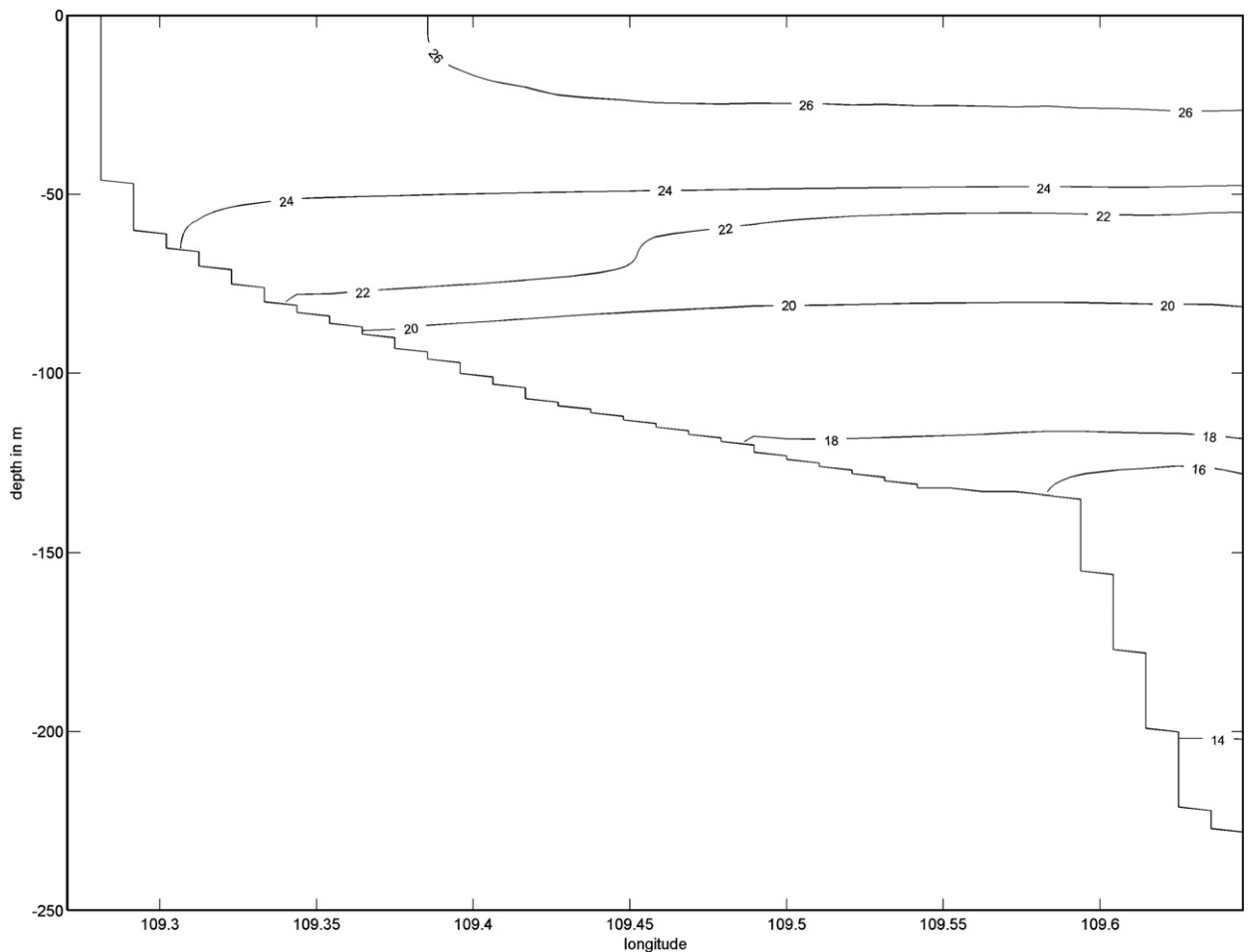


Fig. 5. Temperature ($^{\circ}\text{C}$) at a vertical section along $11^{\circ}52'30''\text{N}$ on 12 December 2004. The figure displays a downwelling situation.

observations (Fig. 9). Even the temporal evolution is captured very well by the model.

Model temperatures are biased high, which may stem from the climatology applied at the boundaries (see Table 2). The climatological values are in fact about 2°C higher than these observations.

The wind forcing data are based on the NCEP data which have a rather coarse resolution (1.9°) compared to the scales we look at. Xie et al. (2003) found that the coastal mountain ridge in Vietnam is responsible for some special features of the wind stress curl that drives the ocean surface circulation of the South China Sea during summer. Wind stress fields with a finer resolution are needed to resolve this mountain effect. The temperature discrepancy found in our results may be a result of local winds that are not resolved by the model.

The seasonal change of hydrography at the open boundary and the seasonal change of winds force the modelled circulation. The circulation pattern agrees well with the large scale circulation, with its regular shift between a south–westerly flow during the dry winter season, to a north–easterly flow during the wet summer season. The southward western boundary current that is present during the whole year (Pohlmann, 1987), is not accounted for in the model. But in the shallow bays the local wind has strong impact on the circulation, so the

neglect of the remotely driven boundary current is assumed to have little effect there. According to Shaw and Chao (1994), Xie et al. (2003) and others, the north–easterly flow diverts offshore at about 12°N , and our results agree well with that (see Fig. 6A). The strong anticyclonic feature in the south is a part of what Xie et al. (2003) call the South Vietnam Eddy.

Table 2

Temperatures from a point at the northern model boundary.

Depth, m	Jan–Mar	Apr–Jun	Jul–Sep	Oct–Dec
0–2	26.15	28.83	27.95	27.01
2–5	26.14	28.79	27.89	27.00
5–10	26.12	28.74	27.83	27.00
10–20	25.97	28.48	27.39	26.88
20–30	25.81	27.85	26.32	26.44
30–50	24.92	25.73	23.81	24.27
50–80	23.10	22.70	21.23	20.90
80–120	20.53	20.34	19.07	18.50
120–200	16.67	17.17	16.38	15.66
200–300	12.90	13.42	12.81	12.85
300–450	10.00	10.31	9.97	9.87
450–615	8.00	8.32	8.07	7.90

The data are interpolated from climatological values (Conkright, 2002), (Levitus, 1982).

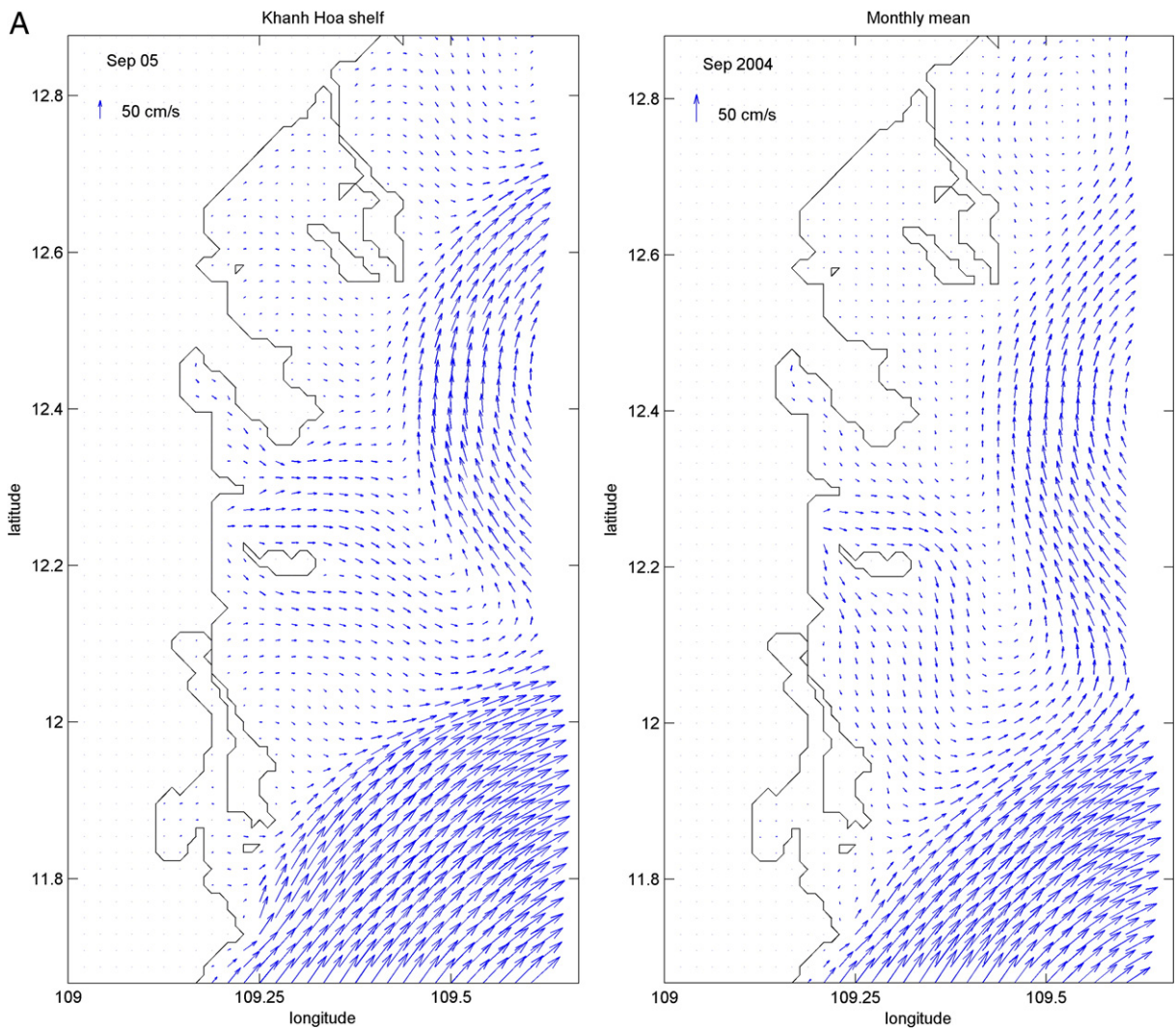


Fig. 6. A. Daily mean surface current (cm/s) of 5 September 2004 (left panel). Monthly mean surface current of September 2004 (right panel). B. Daily mean surface current (cm/s) of 5 September 2004 in Nha Trang Bay (left panel) and Van Phong Bay (right panel). C. Daily mean surface current (cm/s) of 5 September 2004 in Nha Phu Bay (left panel) and Cam Ranh Bay (right panel). (The currents outside Cam Ranh Bay, which are much stronger, have been set to zero to get a view of the field inside the bay.) D. Vertical mean current of 5 September 2004 (left panel). Monthly mean of the vertical mean current of September 2004 (right panel). E. Vertical mean current of 5 September 2004 in Nha Trang Bay (left panel) and Van Phong Bay (right panel). F. Vertical mean current of 5 September 2004 in Nha Phu Bay (left panel) and Cam Ranh Bay (right panel). (The currents outside Cam Ranh Bay, which are much stronger, have been set to zero to get a view of the field inside the bay.)

The south-westerly flow during winter follows the coast (see Fig. 4A), as stated in Shaw and Chao (1994). The Cai river discharge is forced to follow the coast southwards during winter, while it heads offshore during summer (compare the left panels of Figs. 4B and 6B). The island Hon Tre complicates the picture, causing a wake effect during winter. If this island were not there, we would probably see a stronger offshore transport of the river plume during winter, as for example is the case of the outflow from the river Ebro in the Balearic Sea, (Davies and Xing, 2001). The summer monsoon creates upwelling as seen in Fig. 7, while downwelling occurs during the dry winter season (Fig. 5). The signals reach depths of about 100 m, which is in agreement with the fact that coastal upwelling or downwelling is a relatively shallow phenomenon that affects depths down to a few hundred meters. The

signals are rather weak, which probably is because the model region is too small to cover all the complicated processes involved in the Vietnamese upwelling area (Dippner et al., 2007).

The carrying capacities, as determined by the flushing times, differ between the various bays. The smallest of the bays considered is the Nha Phu Bay, with a volume of 0.541 km^3 , which is flushed in only 4.5 days. This is based on the tidally resolved currents. A calculation based on the residual currents (tidal effect averaged out) gives a flushing time of 5.2 days (not shown). The small difference owes to the fact that the tides are small in the Khanh Hoa region, as illustrated by Fig. 15 showing the tidally resolved and residual transports in the upper layer at a point in the opening of Nha Phu bay.

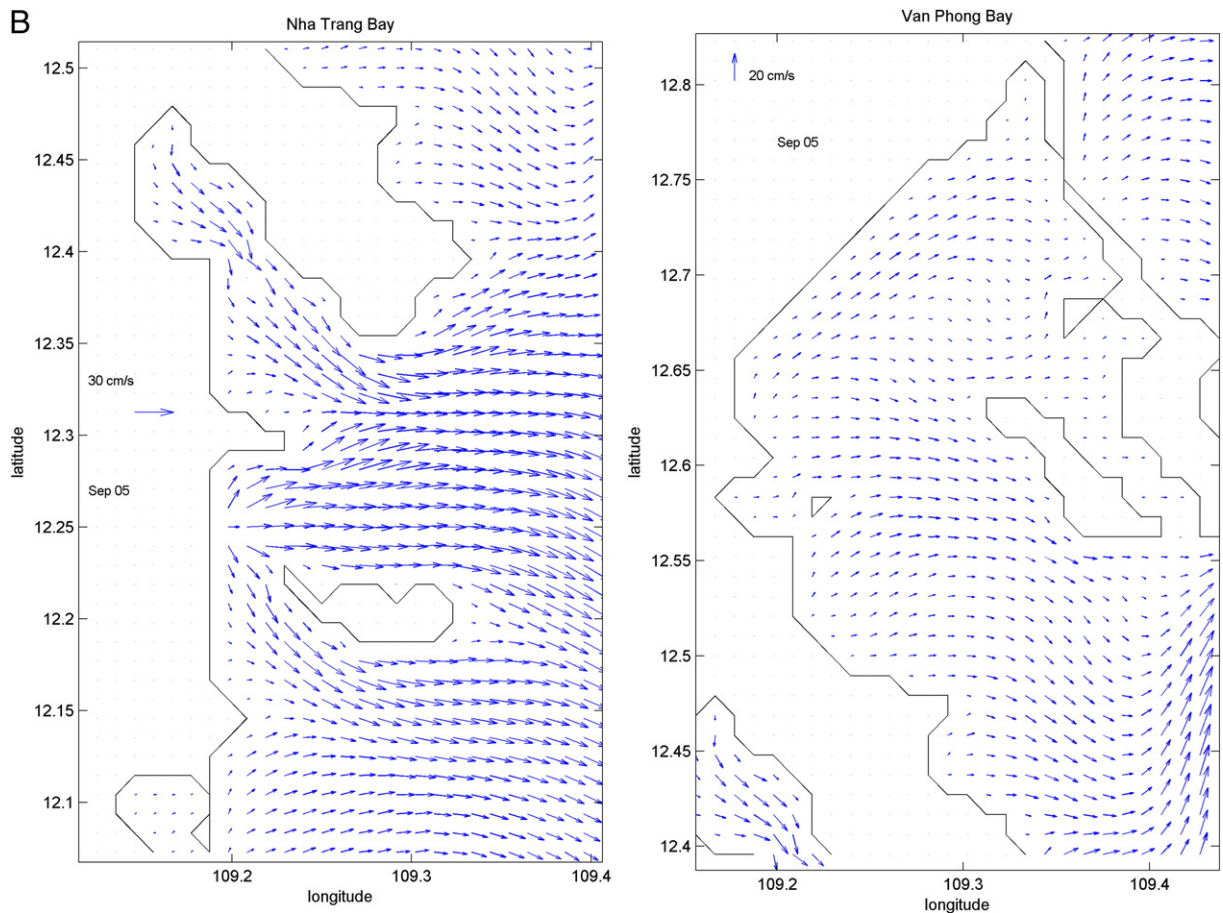


Fig. 6 (continued).

The semi-enclosed Cam Ranh Bay needs 6 days to flush its volume of 1.719 km^3 and 7 days if the calculation is based on the residual flow. A similar volume (1.838 km^3) of the inner part of Van Phong Bay needs 9 days, or 12.5 days if based on the residual flow. Thus the tidal effect is largest in the inner Van Phong Bay, but still this bay has less capacity than Cam Ranh Bay. However, if we do the calculations with the boundary at the narrow opening of Cam Ranh Bay, we find that the flushing times increase to 13 days and 52 days for the tidally resolved and residual flows, respectively.

An and Thu (2007) report in their Table 5 on residence times for Van Phong Bay equal to 61 days in the dry season and 43 days in the rainy season. They do not define the open boundary of the bay. Their estimates are quite large compared to ours, but ours are lower limit estimates for which we assume that the in-flowing water becomes fully mixed before it leaves the bay.

The seasonal variation of the flushing times is influenced by the river runoff and the winds, as well as the open boundary forcing. In Nha Phu Bay the shortest flushing time is in June to August when the wind is from southwest (see Fig. 3), and the river runoff is increasing (confer Table 1). The longest flushing times are found close to the turnings of the monsoon in April and October. The situation is different in

Van Phong Bay and Cam Ranh Bay, where there are no rivers modelled. There the longest flushing times are in July, and the shortest in January and December. In Cam Ranh Bay there are peaks in flushing time also during the turning of the monsoon. The open boundary forcing supports the monsoonal shift as is revealed in Fig. 16 showing time series of surface currents at three selected points along the open boundary of the model domain. The long term mean of the flow at the boundary is determined by the long term mean of the hydrography at the boundary which is prescribed by climatological values.

As the boundary values and the river runoff are climatologic, the meteorological forcing should be for a year that is close to an average. The year 2004 is such an average year, as it is neither an El Nino year, nor a La Nina year, see (Dippner et al., 2007) and their Fig. 15. The error caused by not having actual discharges from 2004 may be felt in the inner Nha Phu bay, which is semi-enclosed and shallow. But the river discharges there are small, so the error should be small.

For aquaculture production the water quality is an important factor, and it depends on the mixing conditions. The model results show that the mixing varies both spatially and temporally. During winter the bays are better mixed than in summer, and outside the bays the winter mixing increases

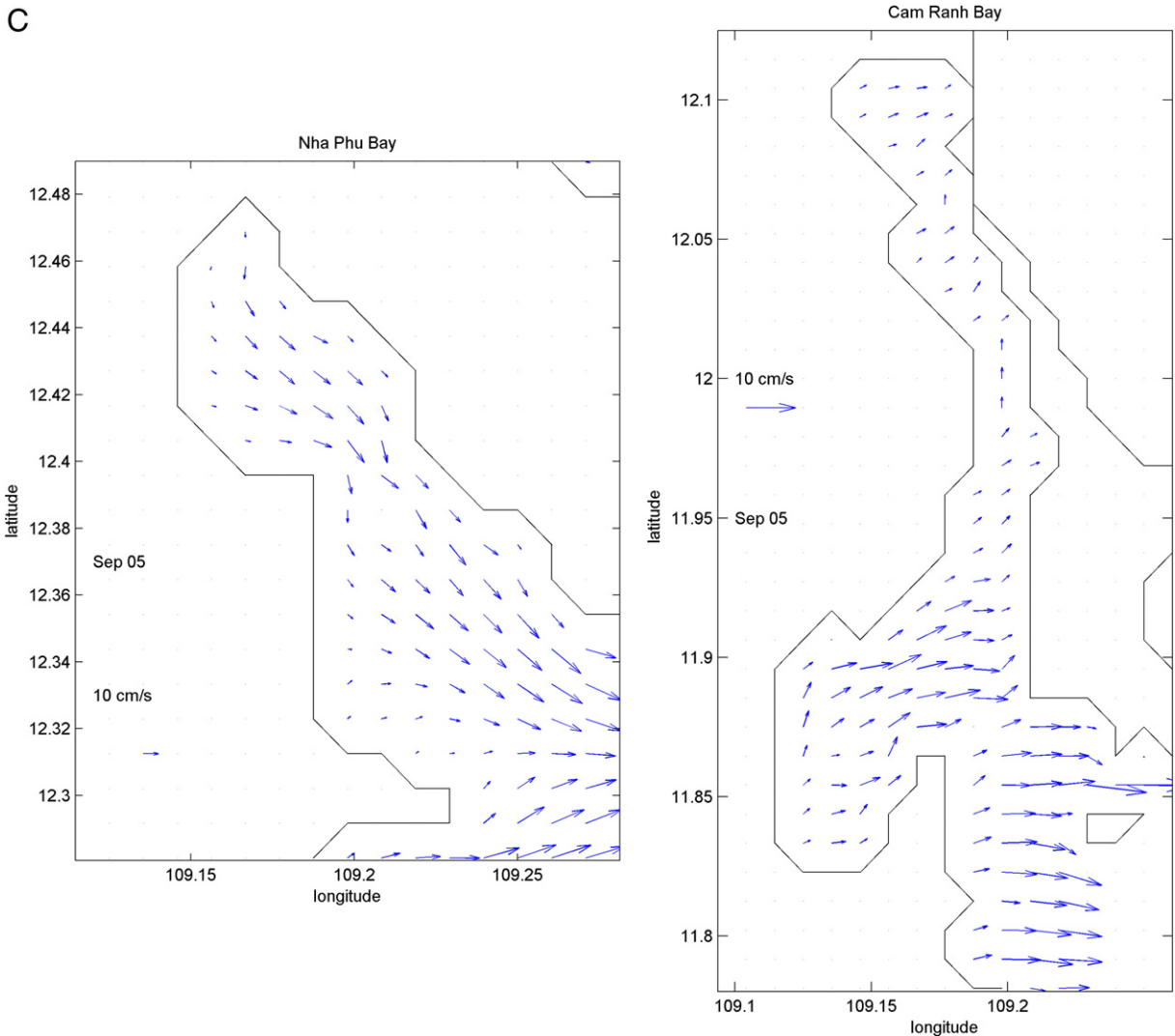


Fig. 6 (continued).

by a factor of ten compared to the summer mixing. The values of the vertical eddy viscosity in Nha Phu Bay are lesser than in the other bays, because the stratification is supported by river water in this bay.

5. Concluding remarks

A three-dimensional ocean circulation model has been implemented on a scale that is sufficiently fine to simulate the exchange of water masses in the bays of Khanh Hoa province, Vietnam. The results can be used to quantify the carrying capacity of the bays. The modelled circulation agrees with the well known monsoonal circulation pattern, but comparison between measured and modelled salinity and temperature reveals some biases. The modelled fields will be applied in a primary production model for the bays. We will for instance examine how the phytoplankton concentration varies with respect to the flushing and mixing conditions in the bays.

Future improvements of the modelling work will include a coupled physical–biological model setup with finer resolution both vertically and horizontally. The atmospheric driving forces will also include diurnal variations. We will also see how to incorporate fine resolution wind stress data.

ENSO has strong impact on the circulation of the South China Sea, (Wu et al., 1998) (Chao et al., 1996). We would like to study interannual variations of the circulation in the bays of Khanh Hoa province, especially the effect of ENSO. But this leaves us with a challenge of how to deal with the temperature and salinity values at the open boundaries during El Nino years.

Acknowledgements

This work has received support from the Norwegian Programme for Development, Research and Higher Education (NUFU) through the grant PRO65/2003, and from the

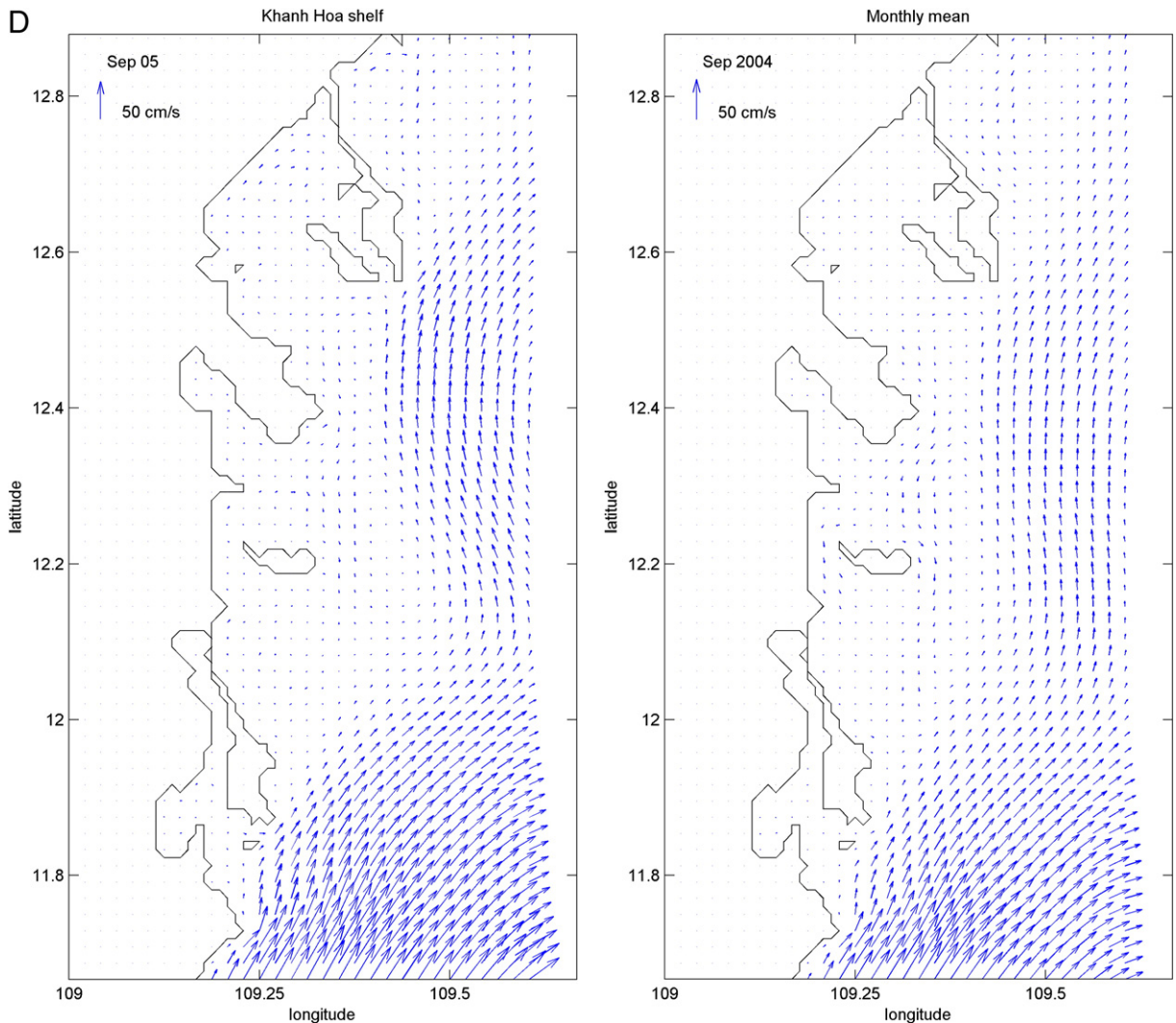


Fig. 6 (continued).

Research Council of Norway (Programme for Supercomputing) through a grant of computing time.

References

- An, N.T., Thu, P.M., 2007. Biogeochemical variability of Vietnamese coastal waters influenced by natural and anthropogenic processes. *Asian Journal of Water, Environment and Pollution* 4 (1), 37–46.
- Backhaus, J.O., 1983. A semi-implicit scheme for the shallow water equations for application to shelf sea modelling. *Continental Shelf Research* 2 (4), 243–254.
- Backhaus, J.O., 1985. A three-dimensional model for the simulation of shelf sea dynamics. *Deutsche Hydrographische Zeitschrift* 38, 174–267.
- Barthel, K., Gade, H.G., Sandal, C.K., 2004. A mechanical energy budget for the North Sea. *Continental Shelf Research* 24 (2), 167–181.
- Bui, H.L., Tran, V.C., 2005. Using tidal harmonic analysis for calculating multi tidal harmonic constants and studying effects of storm surge on sea level in Nha Trang Bay. 1 (T.5). Vietnamese Academy of Science and Technology, Hanoi.
- Chao, S.-Y., Shaw, P.-T., Wu, S.Y., 1996. El Niño modulation of the South China Sea circulation. *Progress in Oceanography* 38 (1), 51–93.
- Conkright, M.E., Locarnini, R.A., Garcia, H.E., O'Brien, T.D., Boyer, T.P., Stephens, C., Antonov, J.I., 2002. *World Ocean Atlas 2001: Objective Analyses, Data Statistics, and Figures*, CD-ROM Documentation. National Oceanographic Data Center, MD, Silver Spring.
- Davies, A.M., Xing, J.X., 2001. Modelling processes influencing shelf edge currents, mixing, across shelf exchange, and sediment movement at the shelf edge. *Dynamics of Atmospheres and Oceans* 34 (2–4), 291–326.
- Dippner, J.W., Nguyen, K.V., Hein, H., Ohde, T., Loick, N., 2007. Monsoon-induced upwelling off the Vietnamese coast. *Ocean Dynamics* 57 (1), 46–62.
- Fofonoff, N.P., Millard Jr., R.C., 1983. Algorithms for computation of fundamental properties of sea water. UNESCO Technical papers in Marine Science 44.
- Hainbucher, D., Hao, W., Pohlmann, T., Sundermann, J., Feng, S.Z., 2004. Variability of the Bohai Sea circulation based on model calculations. *Journal of Marine Systems* 44 (3–4), 153–174.
- Hirtzler, J.D., 1985. Relief of the Surface of the Earth. MGG, 2. National Geographic Data Center, Boulder, CO, USA.
- Kalnay, E., et al., 1996. The NCEP/NCAR 40 year reanalysis project. *Bulletin of the American Meteorological Society* 77 (3), 437–471.
- Kochergin, V.P., 1987. Three-dimensional prognostic models. In: Heaps, N. (Ed.), *Three-Dimensional Coastal Ocean Models*. Coast. estuar. Sci. AGU, Washington D.C., pp. 201–208.
- Levitus, S.E., 1982. *Climatological atlas of the world ocean*, NOAA Professional Paper 13. US Government Printing Office, Washington DC.
- Liu, Z.Y., Yang, H.J., Liu, Q.Y., 2001. Regional dynamics of seasonal variability in the South China Sea. *Journal of Physical Oceanography* 31 (1), 272–284.
- Mellor, G.L., Yamada, T., 1974. Hierarchy of turbulence closure models for planetary boundary-layers. *Journal of the Atmospheric Sciences* 31 (7), 1791–1806.

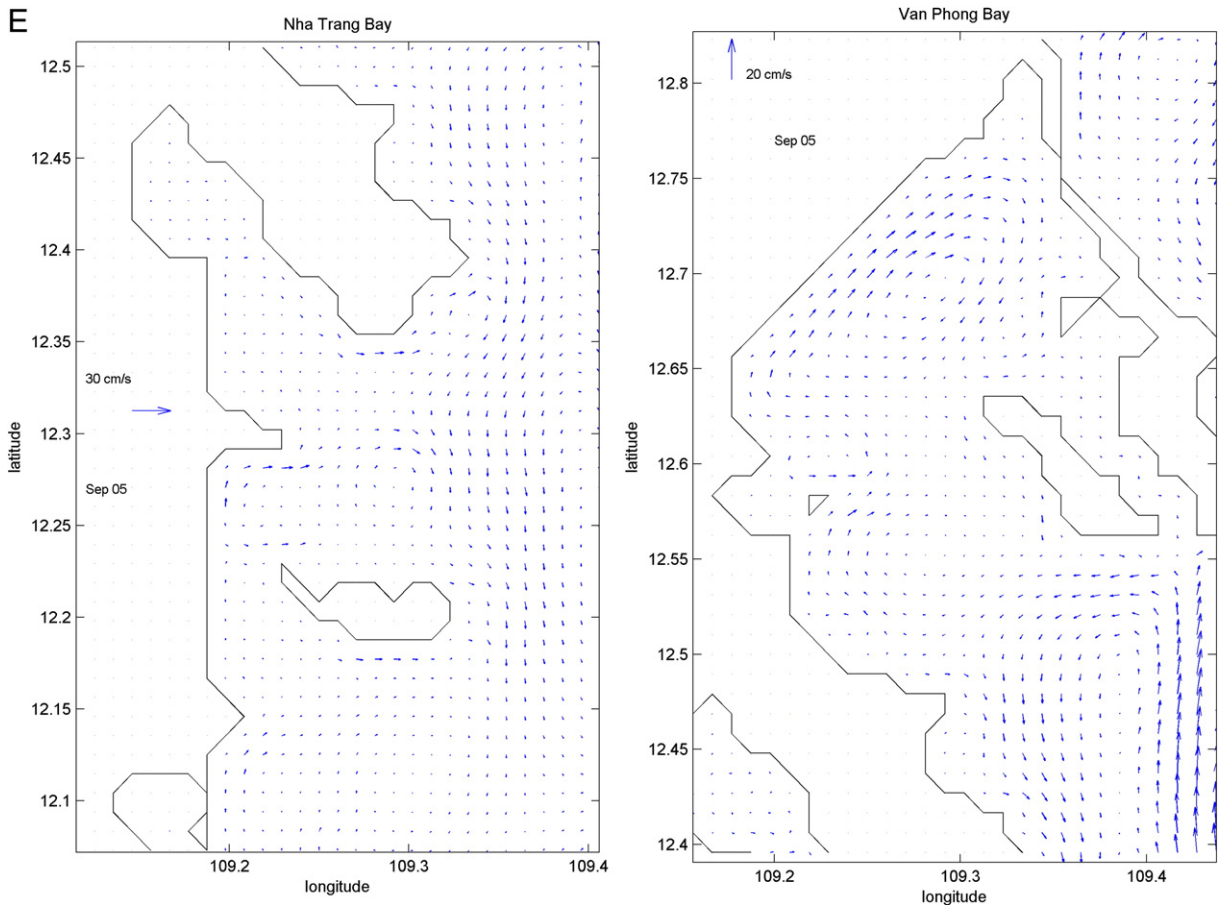


Fig. 6 (continued).

- Pohlmann, T., 1987. A three-dimensional model of the South China Sea. In: Jamart, N.A. (Ed.), *Three-dimensional models of marine and estuarine dynamics*. Elsevier Oceanographic Series, pp. 245–268.
- Pohlmann, T., 1996. Calculating the annual cycle of the vertical eddy viscosity in the North Sea with a three-dimensional baroclinic shelf sea circulation model. *Continental Shelf Research* 16 (2), 147–161.
- Schrum, C., 1997. Thermohaline stratification and instabilities at tidal mixing fronts: results of an eddy resolving model for the German Bight. *Continental Shelf Research* 17 (6), 689–716.
- Shaw, P.T., Chao, S.Y., 1994. Surface circulation in the South China Sea. *Deep-Sea Research Part I-Oceanographic Research Papers* 41 (11–12), 1663–1683.

- Thai, N.C., Rosland, R., Barthel, K. and Bui, H.L., submitted for publication. Modelling nutrient cycling and phytoplankton production at the coast of southern central Vietnam. *Journal of Marine Systems*.
- Wu, C.R., Shaw, P.T., Chao, S.Y., 1998. Seasonal and interannual variations in the velocity field of the South China Sea. *Journal of oceanography* 54 (4), 361.
- Wyrtki, K., 1961. *Physical oceanography of the Southeast Asian Waters*. Scripps Institution of Oceanography. Naga Report., 2. 195 pp.
- Xie, S.P., Xie, Q., Wang, D.X., Liu, W.T., 2003. Summer upwelling in the South China Sea and its role in regional climate variations. *Journal of Geophysical Research-Oceans* 108 (C8).

F

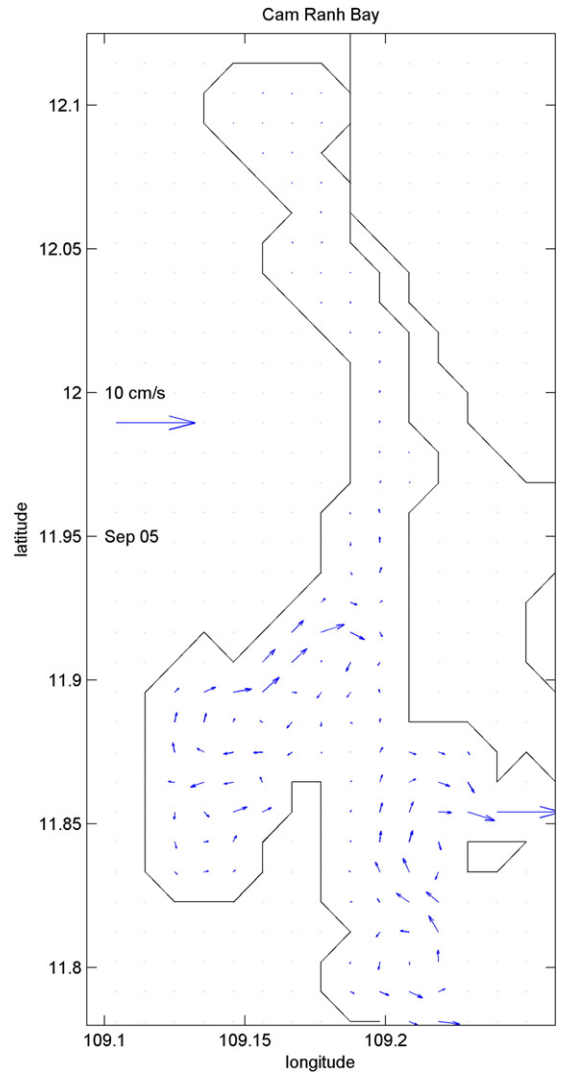
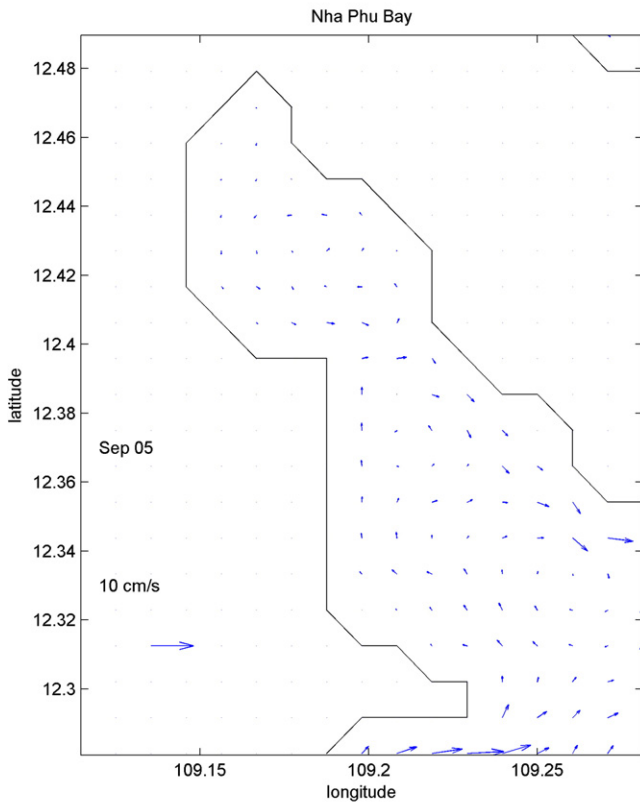


Fig. 6 (continued).

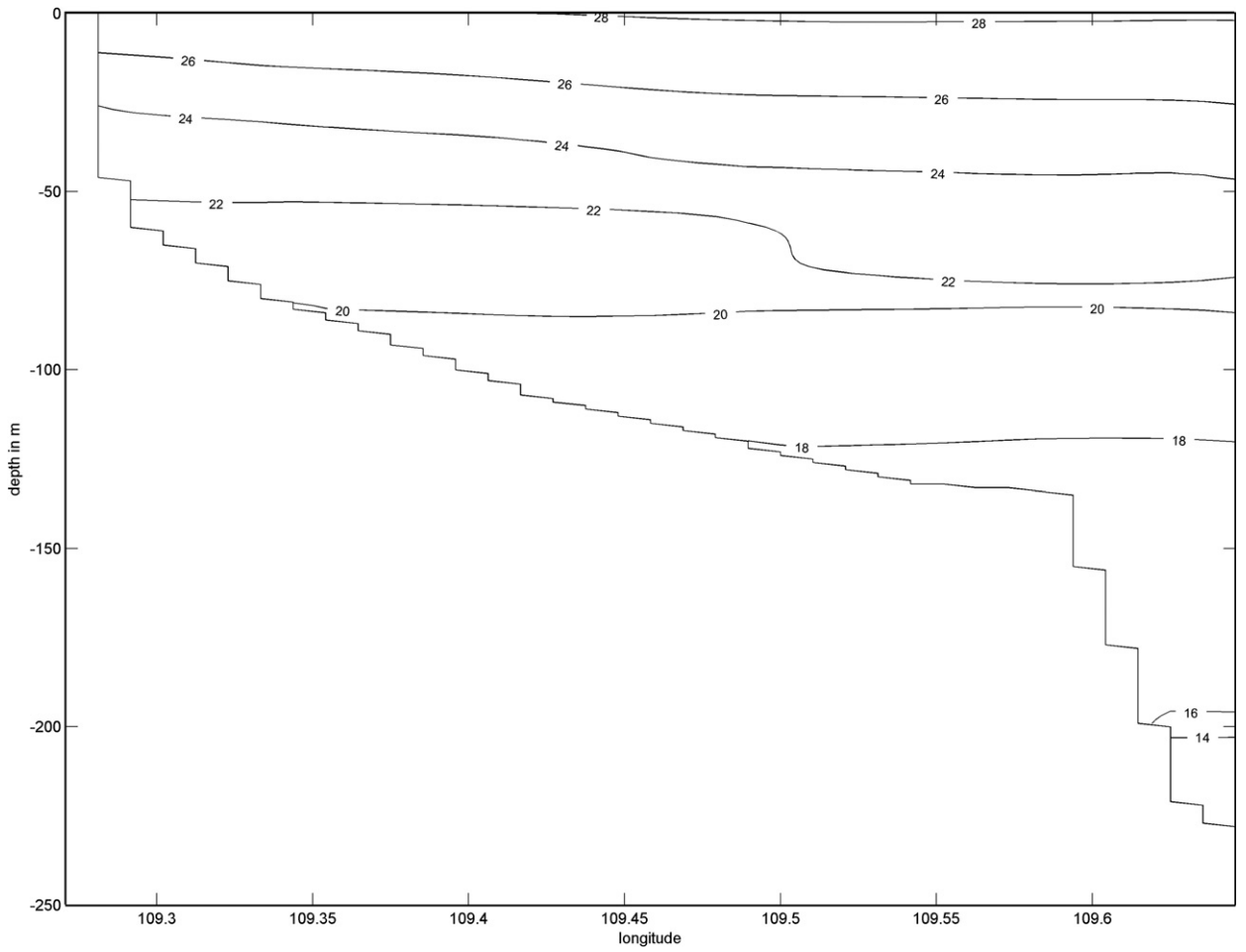


Fig. 7. Temperature (°C) at a vertical section along 11°52'30"N on 5 September 2004. The figure displays a situation of upwelling.

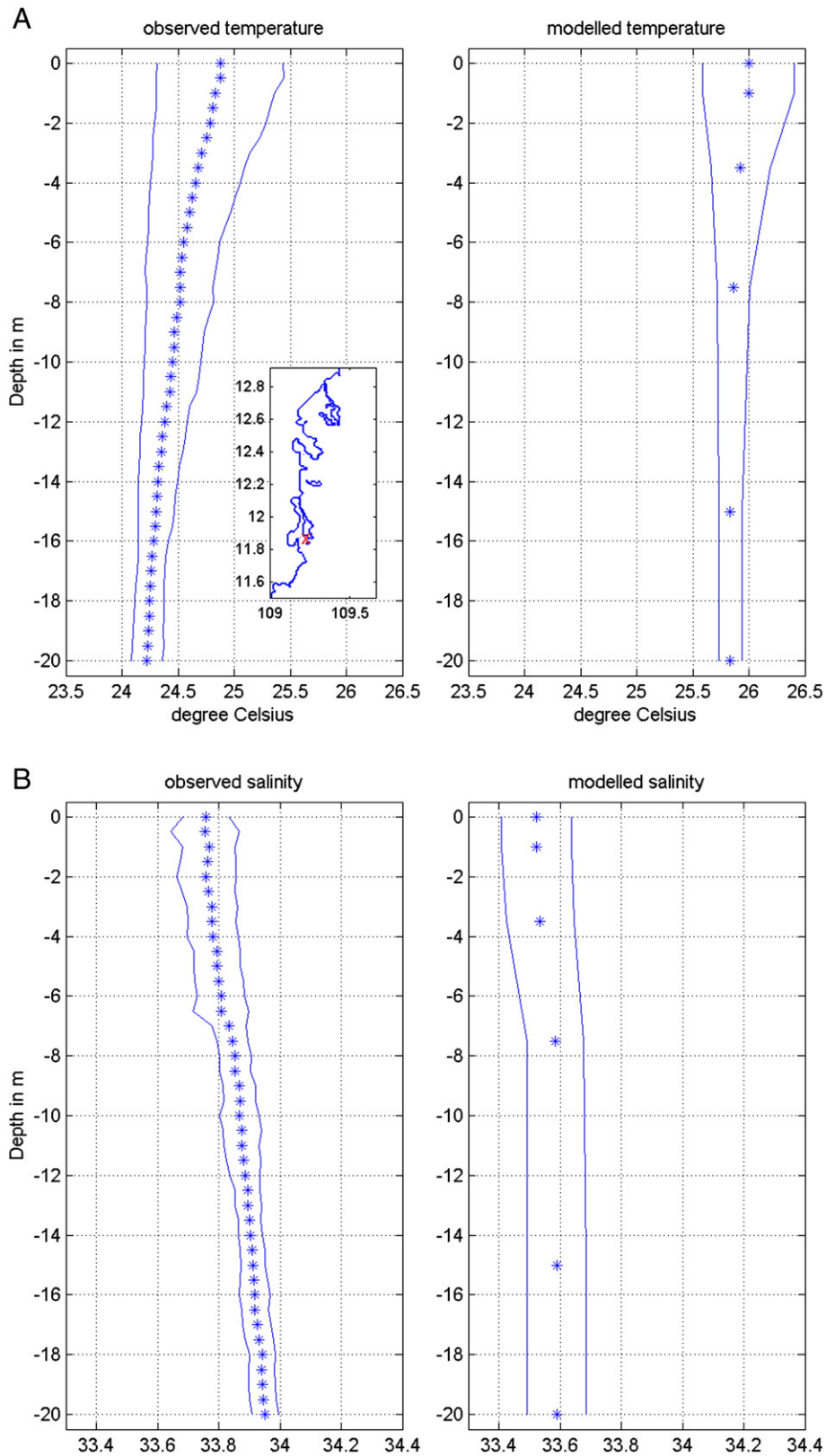


Fig. 8. A. Vertical profiles of mean temperature during the period 9 to 12 March 2004 at the mouth of Cam Ranh Bay, 109°12'04"E, 11°52'26"N. Location is marked with x in the inserted map. The full lines indicate one standard deviation. (Measured data left panel, model results right panel.) B. Vertical profiles of mean salinity during the same period and location. The full lines indicate one standard deviation. (Measured data left panel, model results right panel.)

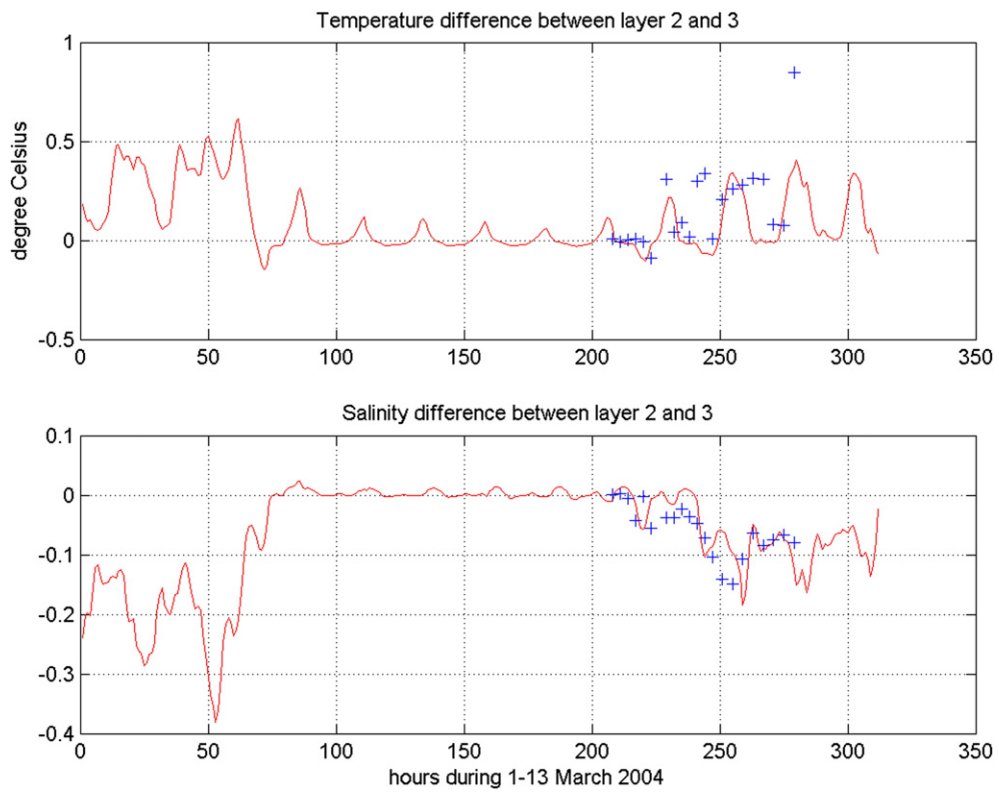


Fig. 9. Time series of modelled (full red curve) and observed (marked with blue +) temperature and salinity difference between 3.5 m and 7.5 m at the mouth of Cam Ranh Bay (see inserted map in Fig. 8a). (For interpretation of the references to colour in this figure legend, the reader is referred to the web version of this article.)

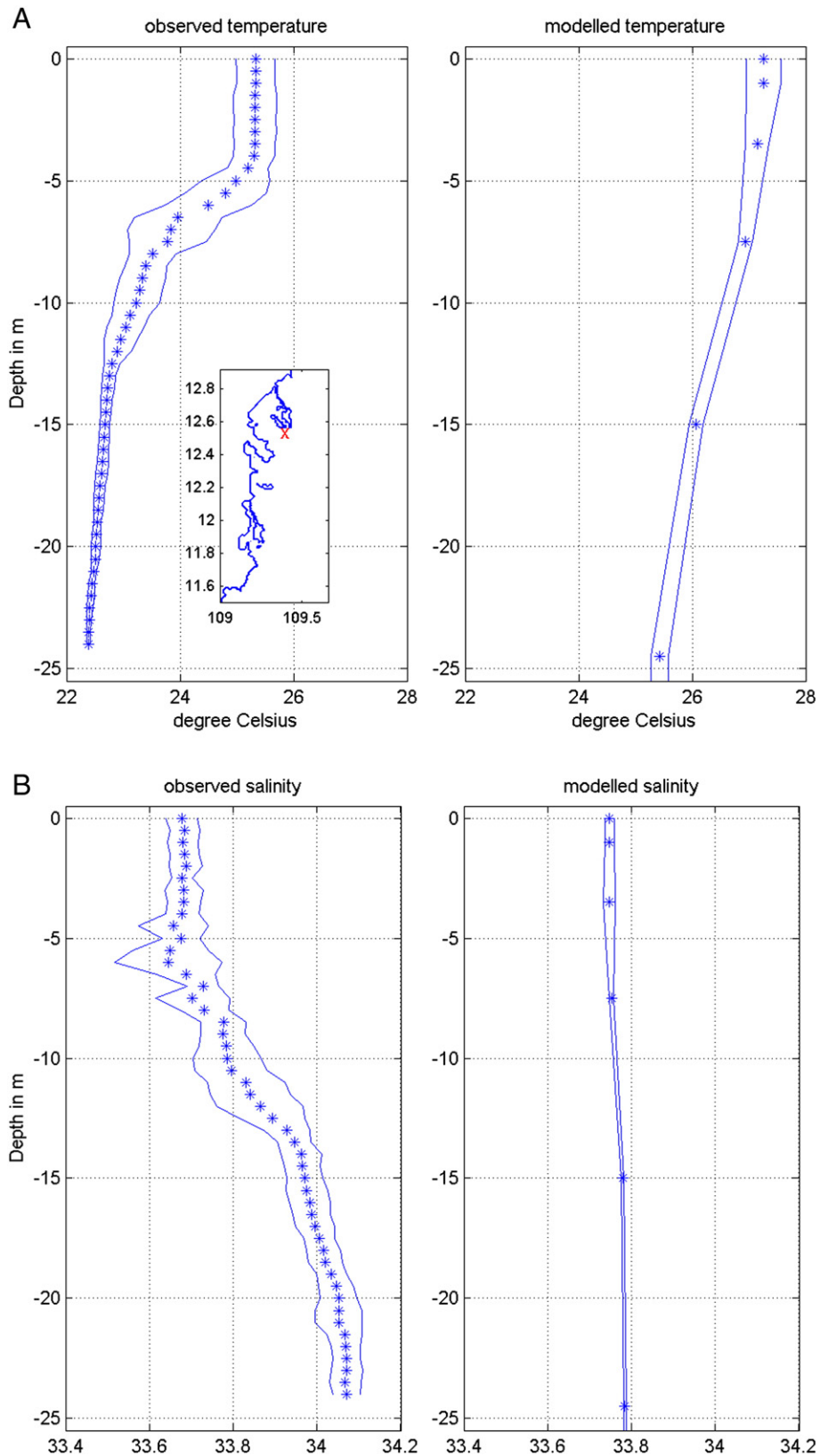


Fig. 10. A. Vertical profiles of mean temperature during the period 2 to 3 March 2004 at the mouth of Van Phong Bay 109°22'29"E, 12°32'08"N. Location is marked with x in the inserted map. The full lines indicate one standard deviation. (Measured data left panel, model results right panel.) B. Vertical profiles of mean salinity during the same period and location. The full lines indicate one standard deviation. (Measured data left panel, model results right panel.)

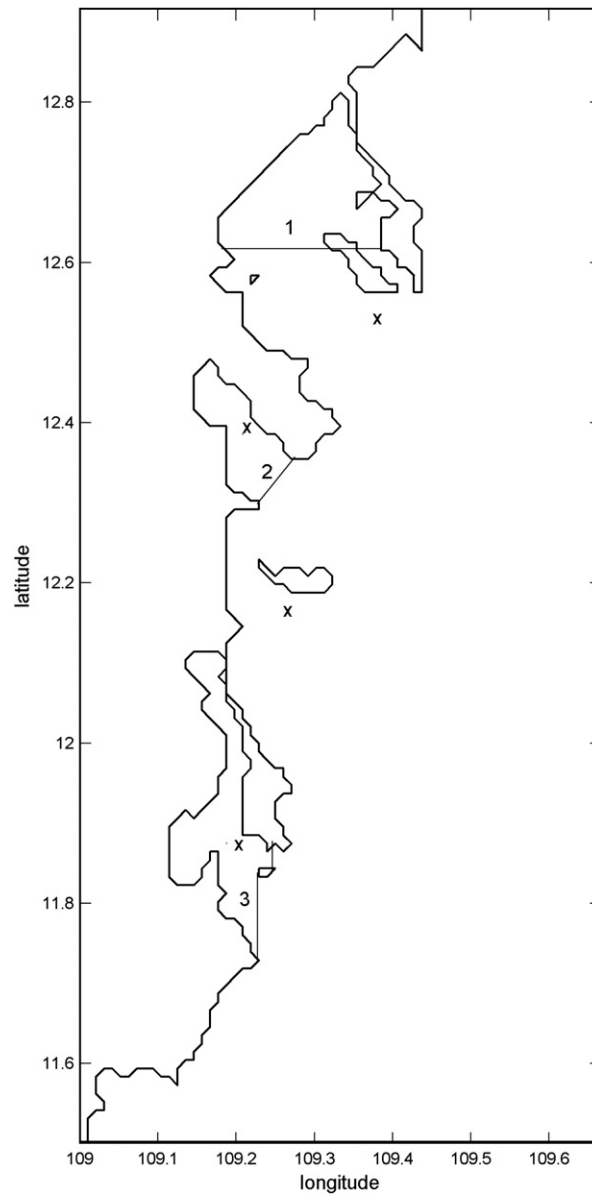


Fig. 11. Open boundaries for the calculation of flushing times in (1) Van Phong Bay, (2) Nha Phu Bay, and (3) Cam Ranh Bay. Positions of time series of daily mean vertical eddy viscosity are marked with 'x'.

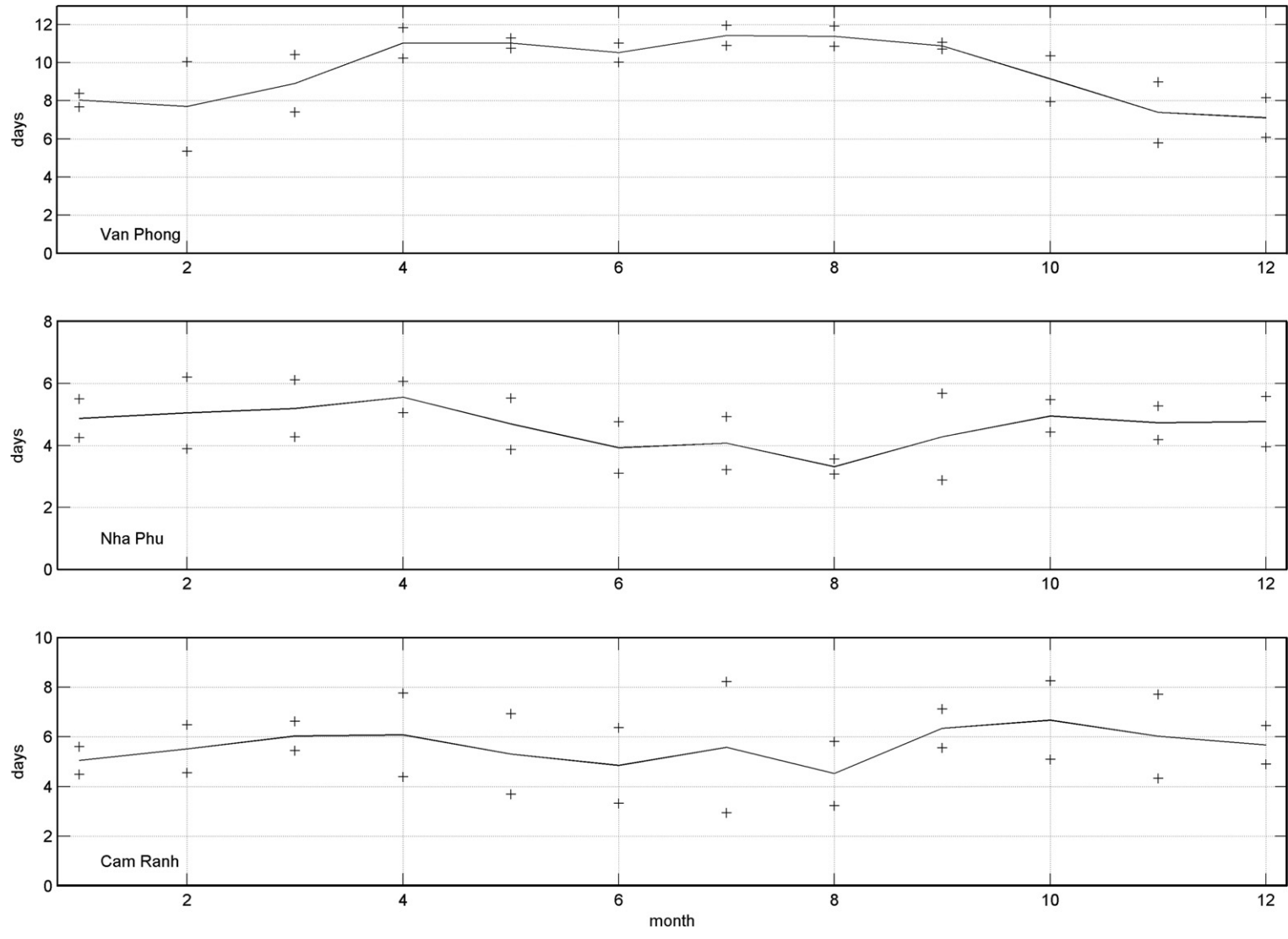


Fig. 12. Monthly mean inflow flushing time for the bays of Van Phong, Nha Phu, and Cam Ranh during 2004. One standard deviation is indicated by '+' signs.

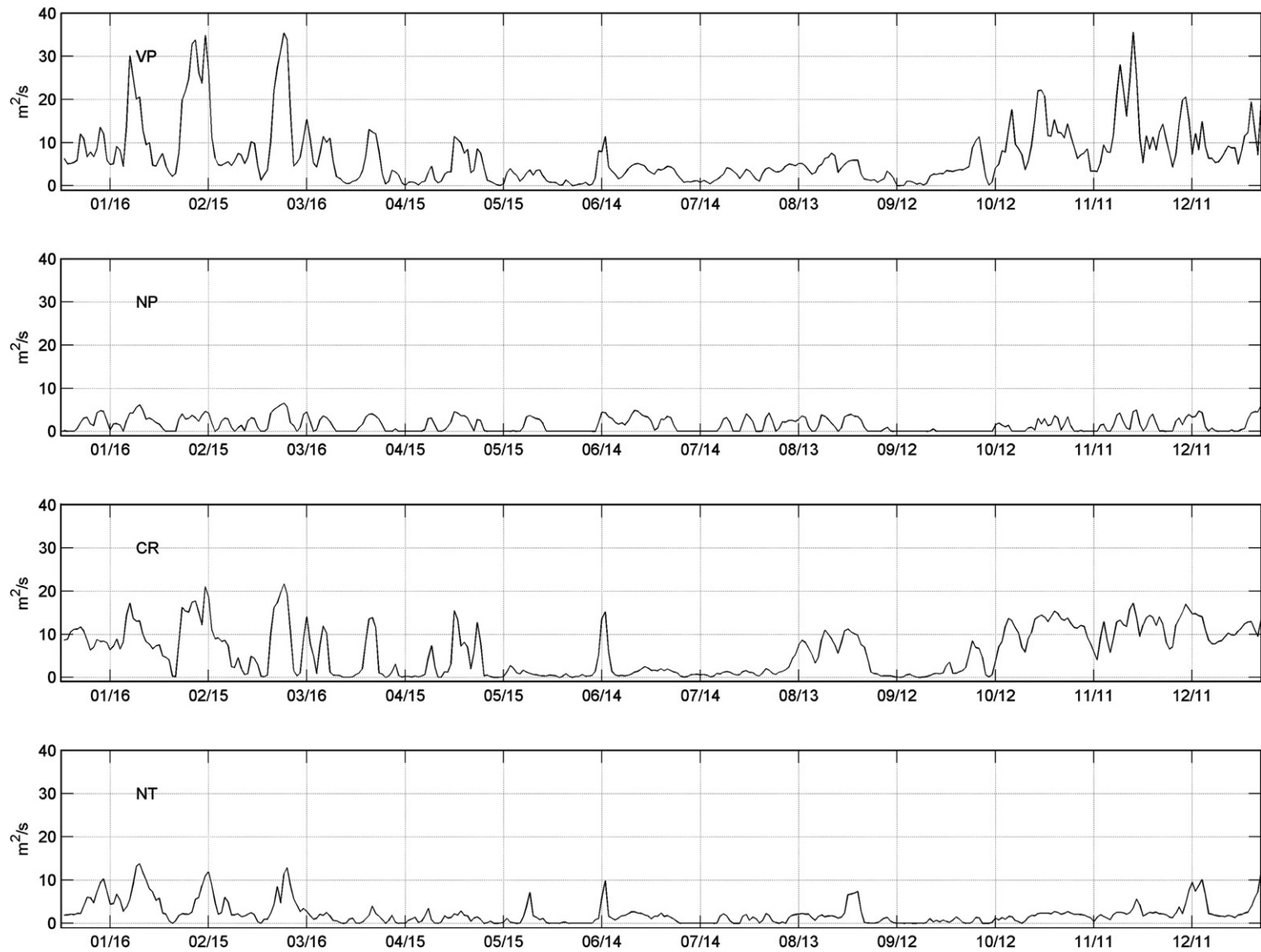


Fig. 13. Daily mean values multiplied by 1000 of vertical eddy viscosity at the mouth of Van Phong bay (upper panel, labelled VP), in Nha Phu bay (second panel, labelled NP), at the mouth of Cam Ranh bay (third panel, labelled CR), and south of the island Hon Tre in Nha Trang bay (lowest panel, labelled NT). The positions are indicated by 'x' signs in Fig. 11.

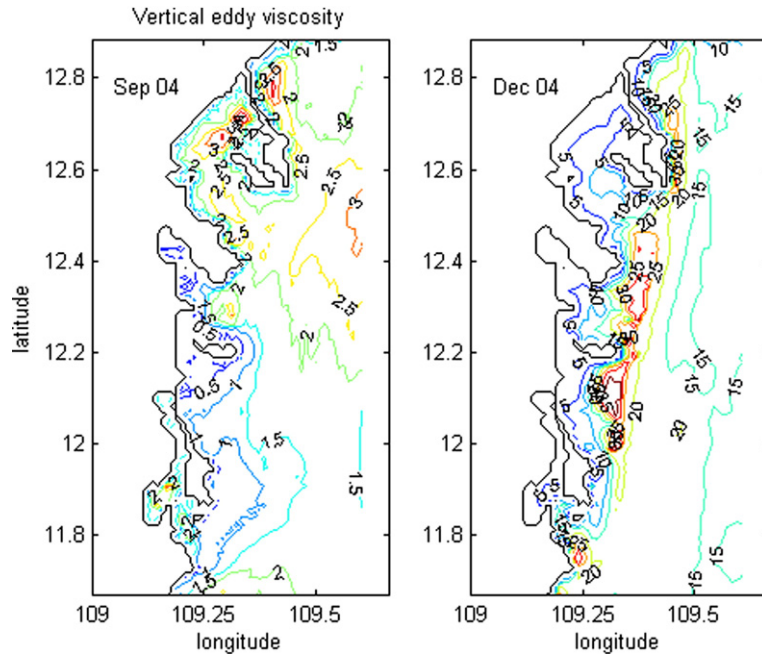


Fig. 14. Monthly mean values multiplied by 1000 of the vertical eddy viscosity (m^2/s) for the summer monsoon season represented by September (left panel), and for the winter season represented by December (right panel).

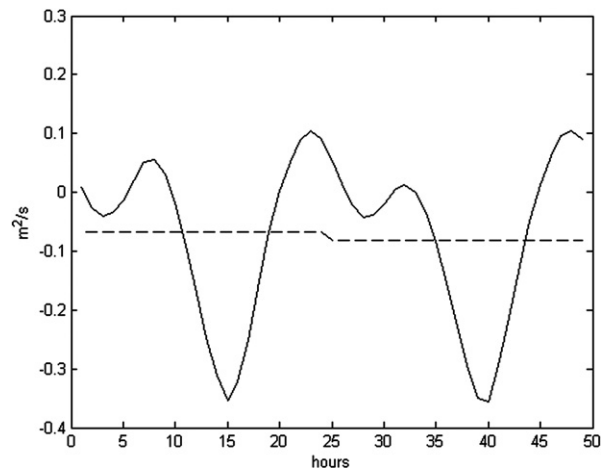


Fig. 15. Tidally resolved transport integrated over the upper 2 m at a grid cell in the opening of Nha Phu bay. The dashed curve gives the corresponding residual transport. A negative value means transport out of the bay.

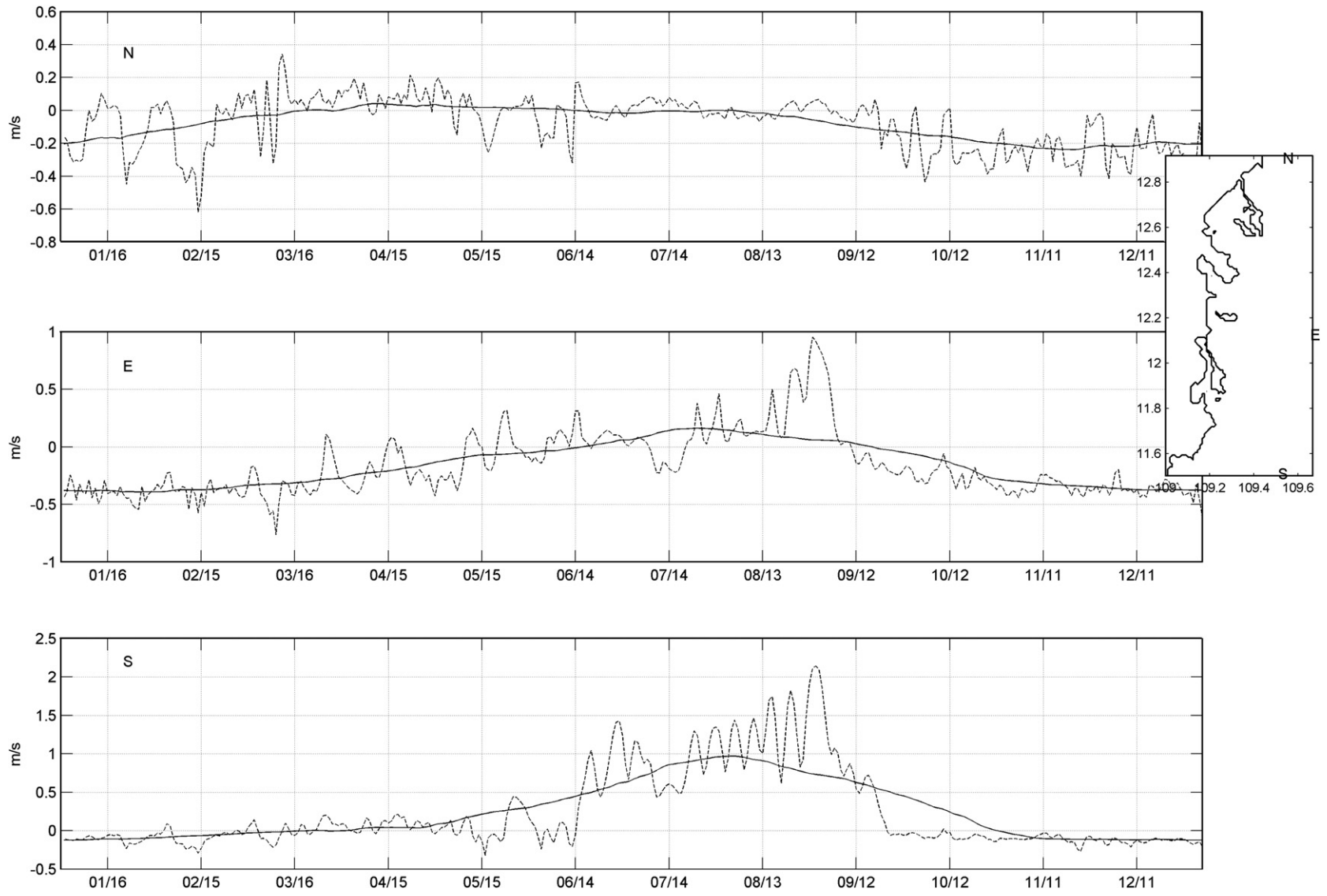


Fig. 16. Time series of 90 days running mean and daily mean (dashed) values of surface current components normal to the open boundary at the locations indicated in the inserted map.